

1. REPORT NUMBER FHWA/CA/SD-81/82	2. GOVERNMENT ASSOCIATION NUMBER	3. RECIPIENT'S CATALOG NUMBER
4. TITLE AND SUBTITLE Fatigue Behavior of Steel Light Poles		5. REPORT DATE December 1981
		6. PERFORMING ORGANIZATION CODE 13-625101
7. AUTHOR John W. Fisher, Roger G. Slutter, Chitoshi Miki		8. PERFORMING ORGANIZATION REPORT NO.
9. PERFORMING ORGANIZATION NAME AND ADDRESS Fritz Engineering Laboratory Lehigh University Bethlehem, Pennsylvania 18015		10. WORK UNIT NUMBER
		11. CONTRACT OR GRANT NUMBER F81RC06
12. SPONSORING AGENCY AND ADDRESS California Department of Transportation P.O. Box 1499 Sacramento, California 95807		13. TYPE OF REPORT AND PERIOD COVERED Final July 1, 1981 to December 31, 1981
		14. SPONSORING AGENCY CODE

15. SUPPLEMENTARY NOTES
 This report was prepared in conjunction with the research project titled "Fatigue Life of Steel Lighting and Signal Standards," in cooperation with the U.S. Department of Transportation, Federal Highway Administration.

16. ABSTRACT
 Standard light poles fabricated to California Department of Transportation standards were tested in fatigue. Comparative results were obtained from testing eight poles fabricated of ASTM A283 Grade D steel and six poles fabricated of ASTM A595 Grade A steel. The first six specimens of ASTM A283 had 45-degree fillet welds at the base of the arm and base of the pole while the ASTM A595 poles had unequal leg fillet welds. Since this difference in geometry affected the fatigue test results, two additional poles were fabricated and tested of ASTM A283 steel with unequal leg welds.

The fatigue strength of the ASTM A283 poles with 45-degree fillet welds was below Category E' while the fatigue strength of ASTM A595 poles with unequal leg weld was equal to Category E'. The two ASTM A283 poles with unequal weld had a fatigues strength equal to Category E. Fatigue cracks appeared at the toe of the weld at the base of the arm and at the base of the pole at approximately the same number of cycles. Cracks were difficult to detect because of the galvanized coating.

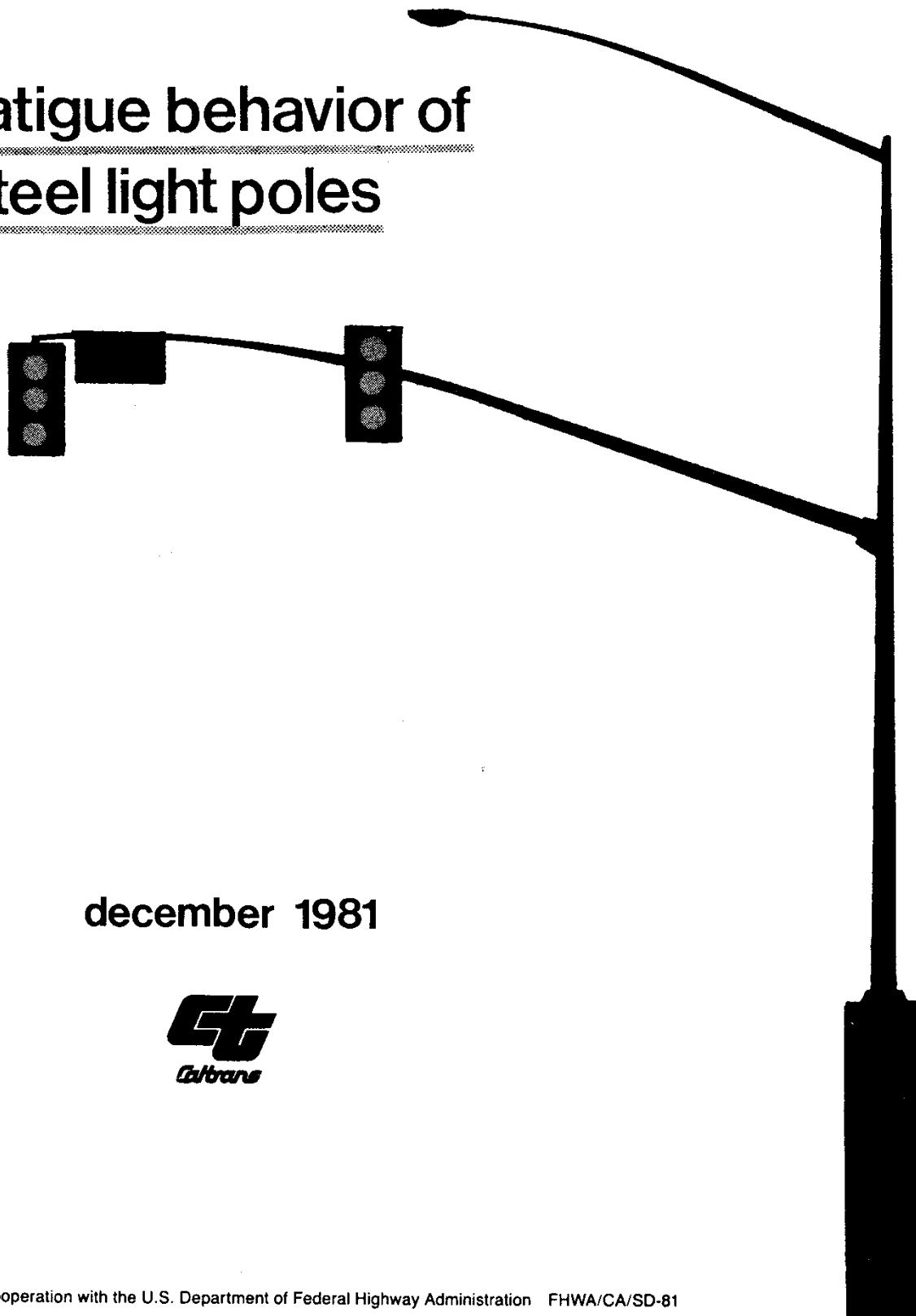
17. KEY WORDS Light poles, fatigue resistance, column fillet welds, fatigue strength	18. DISTRIBUTION STATEMENT no restrictions. This publication is available through the National Technical Information Service, Springfield, Virginia 22161.
19. SECURITY CLASSIFICATION (of this report) unclassified	20. NUMBER OF PAGES 80
	21. COST OF REPORT CHARGED

DISCLAIMER STATEMENT

This document is disseminated in the interest of information exchange. The contents of this report reflect the views of the authors who are responsible for the facts and accuracy of the data presented herein. The contents do not necessarily reflect the official views or policies of the State of California or the Federal Highway Administration. This publication does not constitute a standard, specification or regulation. This report does not constitute an endorsement by the Department of any product described herein.

For individuals with sensory disabilities, this document is available in Braille, large print, audiocassette, or compact disk. To obtain a copy of this document in one of these alternate formats, please contact: the Division of Research and Innovation, MS-83, California Department of Transportation, P.O. Box 942873, Sacramento, CA 94273-0001.

fatigue behavior of steel light poles



december 1981



FINANCIAL DISCLOSURE

This research was jointly funded by the State of California, Department of Transportation, and the Federal Highway Administration. The total amount for this contract, SA E 13915, was \$21,680.

FATIGUE BEHAVIOR OF STEEL LIGHT POLES

by

Chitoshi Miki

John W. Fisher

Roger G. Slutter

This report has been prepared for, and in cooperation with, both the U. S. Department of Transportation, Federal Highway Administration, and the California Department of Transportation.

The contents of this report reflect the views of the authors who are responsible for the facts and the accuracy of the data presented herein. The contents do not necessarily reflect the official views or policies of the STATE OF CALIFORNIA or the FEDERAL HIGHWAY ADMINISTRATION. This report does not constitute a standard, specification, or regulation.

Lehigh University

Bethlehem, Pa.

Fritz Engineering Laboratory Report No. 200.81.714.1

TABLE OF CONTENTS

	Page
1. INTRODUCTION	1
2. DESCRIPTION OF THE TEST SPECIMENS	3
3. TEST PROCEDURE	5
4. RESULTS OF STATIC LOAD TESTS	8
5. FATIGUE TEST RESULTS	10
6. CRACK INITIATION AND PROPAGATION AT WELD TOES	14
7. SUMMARY AND CONCLUSIONS	17
8. IMPLEMENTATION	20
ACKNOWLEDGMENTS	21
REFERENCES	22
TABLES	23
FIGURES	25
APPENDIX I	65
APPENDIX II - STRESS ANALYSIS OF POLES	68

LIST OF TABLES

Table		Page
1	STRAIN MEASUREMENTS - SPECIMEN V4 STATIC LOAD TEST	23
2	SUMMARY OF FATIGUE TEST RESULTS	24

LIST OF FIGURES

Figure		Page
1	Specimen Geometry	25
1b	Summary of Weld Details	26
2	Location of Seam Welds on Pipe Arm and Column	27
3	Typical Fillet Weld Profiles for Pipe Arm and Column Base of A Series of Specimens (A1 to A6)	28
4	Typical Fillet Weld Profiles for Pipe Arm and Column Base of V Series Specimens	29
5	Typical Fillet Weld Profiles for Pipe Arm and Column Base of Specimens A7 and A8	30
6	Test Setup	31
7	Testing Setup	32
8	Location of Strain Gages and Dial Gages	33
9	Measured Strain versus Load for Specimen A1	34
10	Measured Load Deflection Behavior of Specimen A1	35
11	Comparison of Measured Strain with Predicted Strain - Specimen A1	36
12	Comparison of Measured Strain in Pipe and Column with Theoretical Strain - Specimen A1	37
13	Load-Deflection and Load-Strain Relationships for Specimen A2	38
14	Load-Deflection and Load-Strain Behavior of Specimen A3	39
15	Load-Deflection and Load-Strain Behavior of Specimen A4	40
16	Load-Deflection and Load-Strain Relationships for Specimen A5	41

LIST OF FIGURES (continued)

Figure		Page
17	Load-Deflection and Load-Strain Relationships for Specimen A6	42
18	Load-Deflection and Load-Strain Relationships for Specimen A7	43
19	Load-Deflection and Load-Strain Relationships for Specimen A8	44
20	Load-Deflection and Load-Strain Behavior of Specimen V1	45
21	Load-Deflection and Load-Strain Response of Specimen V2	46
22	Load-Deflection and Load-Strain Response of Specimen V3	47
23	Load-Deflection and Load-Strain Behavior of Specimen V4	48
24	Load-Deflection and Load-Strain Behavior of Specimen V5	49
25	Load-Deflection and Load-Strain Behavior of Specimen V6	50
26	Location of Strain Gages on Pipe Arm of Specimen V4	51
27	Load-Strain Response Around Pipe Arm - Specimen V4	52
28	Comparison of Measured Strain Distribution with Theoretical Distribution, Specimen V4	53
29	Typical Crack at Weld Toe on Pipe Arm	54
30	Summary of Stress Range versus Cycle Life for A and V Series	55
31	Crack Surface of Specimen A1	56

LIST OF FIGURES (continued)

Figure		Page
32	Crack Surfaces of Specimen A5	57
33	Crack Surfaces of Specimen A7	58
34	Crack Surfaces of Specimen V4	59
35	Crack Surfaces of Specimen V5	60
36	Crack Shape at Various Cycle Life Intervals – Specimen A5	61
37	Crack Shape at Various Cycle Life Intervals – Specimen V4	62
38	Fatigue Crack Detected at the Pipe Arm Weld Toe of Specimen V6	63
39	Small Fatigue Cracks at the Column Base Weld Toe of Specimen V4	63
40	Small Fatigue Crack at the Column Base Weld Toe of Specimen A6	64

1. INTRODUCTION

In order to assess the comparative performance of two types of standard light poles, fatigue tests were carried out on a series fabricated from A283 Grade D steel and on a series fabricated from A595 Grade A steel. The test specimens were designed and proportioned by California Department of Transportation.

The specimens fabricated from A283 Grade D steel poles were built by Ameron Pole Products Division. The specimens fabricated from A595 Grade A steel poles were built by Valmont Industries.

Six specimens were initially provided for each grade of steel. The specimens fabricated from A283 Grade D steel had the standard 45° equal leg fillet weld connecting the poles to the plates. The specimens fabricated from A595 Grade A steel were found to have unequal leg fillet welds. Two additional specimens were fabricated from A283 Grade D steel and furnished for testing by Ameron when it was discovered that the poles with unequal leg fillet welds connecting the pipes to the heavy rectangular base plates had better fatigue resistance than equal leg fillet welds. The two additional specimens fabricated from A283 Grade D steel were also provided with unequal leg fillet welds similar to the specimens furnished from A595 Grade A steel. Photographs of the weld profiles are provided and illustrate the differences in geometric conditions at the weld toe. The results of these additional tests are included in this report.

200.81.714.1

It was not known at the time the tests were initiated what fatigue category was applicable to the pipe-plate connection. The existing specification provisions provided by AASHTO did not define this type connection.⁽¹⁾ No test data was known to be available for this type of connection.

2. DESCRIPTION OF THE TEST SPECIMENS

Figure 1 shows the elevation of the two types of test specimens for the initial test series. The geometric proportions of the 40 and 48 series specimens were the same except for the wall thickness of the tubes and the size of the fillet welds connecting the tubes to the arm connection plates and to the base plates. Appendix I shows the design drawings for the two test series. The fillet weld details that were furnished are shown in Fig. 1b.

The 40 series specimens were designated for identification as Specimens A1 to A6. All six of these specimens were fabricated with the longitudinal pipe seams positioned in the manner shown in Fig. 2. This placed the seam for the pipe arms at the top of the connection and for the pipe columns at the inside edge.

The 48 series specimens were designated as V1 to V6. The pipe weld seams appeared to be randomly placed and their locations at the arm connection plates and base plates are also shown in Fig. 2.

The bending stress at the arm connection (identified as Sect. I in Fig. 1) and at the column base connection (identified as Sect. II in Fig. 1) were nearly equal for each series of test specimens. The axial stresses introduced into the pipe arm and column were small in comparison with the bending stress. Appendix II provides details of the stress analysis.

After testing was completed, the connections were cut from the assembly in order to expose the fatigue cracks and to provide cross sections of the weld profiles. Figure 3 shows typical fillet weld profiles of the arm and base connections that were furnished for the 40 series specimens (A1 to A6). These weldments were all equal legs as indicated on the design drawings (see Fig. 1). Figure 4 shows typical fillet weld profiles of the arm and base connections for the 48 series specimens (V1 to V6). These weldments were all unequal leg fillet welds with the long leg on the pipe arm or column.

The two supplemental test specimens A7 and A8 were also furnished with unequal leg fillet welds. These weld profiles are shown in Fig. 5 and are similar to the 48 series test specimens.

The material properties provided from the mill reports indicated that A283 Grade D pipe had a yield point of 46.5 ksi and a tensile strength of 65.5 ksi.

The A595 Grade A pipe had an average yield point of 61.7 ksi and a tensile strength of 73.3 ksi.

3. TEST PROCEDURE

All specimens were tested on the dynamic test bed as shown schematically in Fig. 6. The test specimens were all bolted to steel plates that were bolted directly to the dynamic test bed floor. A test frame was erected and a 22 kip Amsler hydraulic jack was suspended from the cross beam. Figure 7 shows a photograph of the specimen mounted for testing. The anchor bolts attaching the plates to the test floor and the bolts attaching the base plates to the larger plates can be seen together with the test frame.

All fatigue tests were carried out at a loading rate of 250 cpm with loads applied by the hydraulic jack and Amsler pulsators. The minimum load for all fatigue tests resulted in a maximum bending stress at sections I and II of about ± 5 ksi. The minimum load was set at 1.5 kips for the 40 series specimens and at 1.2 kips for the 48 series specimens.

The first two test specimens were tested at a stress range of about 19 ksi at Sections I and II. This resulted in a maximum load of 7.1 kips for the 40 series specimen and 5.6 kips for the 48 series specimen. These stress levels were selected as it was not known which fatigue design category was applicable to the welded connections. The stress range selected was thought to provide a cyclic life less than 500,000 cycles. Because failure occurred at less than 100,000 cycles for both test specimens, subsequent tests were carried out at stress

range levels of about 6.5 and 12.5 ksi. This corresponded to a maximum load of 3.4 kips and 5.2 kips for the 40 series specimens and 2.7 kips and 4.1 kips for the 48 series specimens.

Electrical resistance strain gages were attached to each test specimen as shown schematically in Fig. 8. A dial gage was also used to measure the deflection of the arm under the test load. Several of these gages can be seen in Fig. 7. Prior to commencing the fatigue test, a static load test was carried out on each test specimen. The increments of strain at the arm and base sections and the arm deflection were recorded at 1 kip intervals during the static load test.

Because of the dynamic response of the specimens, a large difference existed between the load dials on the testing machine and the static loads. In order to provide the correct cyclic stress conditions the minimum and maximum deflection were controlled and made equal to the static load increments. The strain range was also checked with a recording oscillograph to insure that the specimens were subjected to the desired stress range.

Failure was defined as the number of stress cycles necessary to activate the limit switch on the maximum load dial. This switch was set to activate when a 2 kip drop in maximum load occurred. This corresponded to a fatigue crack that severed about half the pipe at either the arm or base plate connection.

The crack front was marked on three specimens (A5, V4, V5) by decreasing the stress range by at least half for a period of 50,000 to

100,000 cycles. This marked the crack front and permitted the crack shape to be delineated during the crack growth stages.

4. RESULTS OF STATIC LOAD TESTS

The strain and deflection readings for the static load tests were summarized and plotted for each test specimen. Load-deflection and load strain plots were prepared. Figures 9 to 25 show the resulting load-deflection and load-strain plots for the fourteen test specimens. Also plotted in the load-strain figures are the theoretical strain for the top and bottom of the arm at Section I.

The results show that the measured strains were in reasonable agreement with the theoretical strain. It should also be noted that the strain in the arm will increase at the weld toe because of the moment gradient in the arm. The strain in the column will decrease slightly at the weld toe because of the increase in pipe diameter and the fact that the column is subjected to a uniform moment along its length.

The figures for the 40 series (A) specimens (Figs. 9 to 19) indicate that the measured strain are slightly lower than the theoretical strain. The measured strain at the arm gages (gages 2 and 4) were slightly higher than the pipe base gages (1 and 3).

The strain measurements on the 48 series (V) specimens were generally closer to the predicted strain. This suggested that the pipe sections were slightly larger than the assumed size for the 40 series tests. All load conditions were established using the measured strain conditions.

One test specimen from the 48 series (specimen V4), was supplied with additional electrical resistance strain gages in order to establish and verify the strain distribution across the pipe section. Figure 26 shows the location of the additional strain gages that were added to the arm.

The results of this special test are summarized in Table 1 and in Fig. 27. Figure 27 shows the load-strain relationship for each strain gage location. Since the strain gaged section was only 1 inch from the weld termination, the calculated strain was based on the properties at Section I.

The strain distribution around each half of the pipe arm is plotted in Fig. 28. The change in strain for a load increase from 1.0 to 4.1 kips and for a load decrease from 4.1 to 1.2 kips show comparable changes for each segment of the pipe arm. The results demonstrate that very little axial stress existed from the applied loads. The theoretical and measured strain gradients were in good agreement.

5. FATIGUE TEST RESULTS

The fatigue test results are summarized in Table 2. The load range, stress range at Sections I and II, measured strain and deflection range, and the cycles to failure are shown for each test specimen. Also listed is the location governing the failure (arm or base) and the size of the fatigue crack detected at the location that did not completely fail.

As is apparent from an examination of Table 2, most failures were at the arm connection. Only two 48 series test specimens failed at the base location (Section II). However, two specimens that did not fail at the base connection still had relatively large fatigue cracks at the time the test was terminated. These base cracks varied in length from 4 to 11 inches along the weld. All cracks were through the pipe thickness so that most if not all of their fatigue resistance was exhausted. The crack lengths were established by liquid penetrant inspection. Figure 29 shows a crack at the fillet weld toe of the pipe arm base connection.

It was observed during the tests that small cracks could not be detected readily because of the existence of the hot-dip galvanized coating. The coating apparently stretched and bridges small cracks without breaking.

The test results are also summarized in Fig. 30. Stress range at the weld toe is plotted as a function of cycle life. The 40 series test specimens (A1 to A6) are seen to provide less fatigue resistance than the 48 series test specimens (V1 to V6). Also plotted in Fig. 30 are the fatigue resistance curves for Categories E and E'. At the high stress range levels (12.5 and 19 ksi) the 40 series test specimens were below Category E. The 48 series specimens corresponded to Category E'. At the 6.5 ksi stress range level the 40 series (A) specimens provided a fatigue strength between 1.2 and 1.9 million cycles which was near the Category E' line. The 48 series (V) specimens provided fatigue lives between 5.2 and 9 million cycles.

It is readily apparent that the weld profile provided on the V series test specimens (see Fig. 4) decreased the stress concentration and increased the fatigue resistance of the 48 series test specimens. Fatigue studies of the fillet weld profile have provided similar increases in fatigue resistance.⁽²⁾ At 2×10^6 cycles, the difference in stress range for a 30° contact angle was 1.5 times as great as a 45° contact angle.

An analytical study by Frank⁽³⁾ provided similar orders of magnitude differences. The analytical crack growth model which was correlated with 45° fillet welds was found to provide increased fatigue life when the weld contact angle was decreased which decreased the stress concentration.

Measurement of the contact angle of the fillet welds shown in Figs. 3, 4 and 5 indicate that the 40 series (A) specimens had a 45°

contact angle and that the 48 series (V) specimens had a 28° contact angle.

As a result of these observations, two additional 40 series specimens (A7 and A8) were fabricated with a comparable weld contact angle. As was illustrated in Fig. 5, the contact angle on the pipe arm where failure occurred was 34°. The column base was 30°.

The two 40 series specimens with a 34° contact angle are plotted in Fig. 30 as specimens A7 and A8. The weld profile change can be seen to increase the fatigue resistance of the 40 series specimens at the 6.5 ksi stress range level to nearly 4×10^6 cycles. This was about one million cycles less than the least life provided by the 48 series tests. A comparison of the weld profiles shown in Figs. 4 and 5 demonstrates that the 48 series test specimens had a smoother transition to the pipe surface. Hence the lesser difference in fatigue resistance between the 40 and 48 series tests with about the same weld profile appears to be due to the profile alone. The location of the longitudinal weld seam does not appear to have a significant effect on the fatigue behavior of the samples.

Decreasing the stress concentration by using unequal leg fillet welds provides a significant improvement in fatigue resistance. An additional improvement may be obtained by either peening the weld toe region on the tubes or by using the gas tungsten arc remelt process to minimize the discontinuities at the weld toe and create a smaller stress concentration. (5)

For the specific pipe geometry tested, the unequal leg A283 Grade D steel specimens provided about the same load range resistance. The difference in section properties is about the same as the difference in the Category E and E' resistance curves.

6. CRACK INITIATION AND PROPAGATION AT WELD TOES

As can be seen in Fig. 29, the fatigue cracks in the pipe arm or column formed at the weld toe. Figures 31 to 35 show typical crack surfaces for several of the fracture locations. Figures 31, 32 and 34 show typical crack surfaces that formed at the pipe arm connection. Figures 33 and 35 show typical crack surfaces that formed at the column base.

Two specimens that had their crack front marked by changing the stress range to create distinctive bench marks are shown in Fig. 32 and 34. Specimen A5 from the 40 series shows failure at the arm as does specimen V4 from the 48 series. Schematic drawings of the crack profile are given in Figs. 36 and 37 for these two specimens. It is apparent that multiple initiation sites occur along the weld toe and coalesce into a wide but shallow surface crack. This condition is comparable to the crack growth conditions observed at other weld toes.⁽⁴⁾ After 45% of the fatigue life was exhausted the semielliptical surface crack was 0.1 in. deep and 2 in. wide in specimen V4. Specimen A5 was found to have a 0.1 in. deep crack 1.1 inches long after 22% of its fatigue life was exhausted. This crack size difference is compatible with the stress these two specimens were subjected to. Specimen A5 had a stress range of 6.4 ksi and specimen V4 was subjected to a stress range of 12.4 ksi. After 75 to 85% of the fatigue life was exhausted the cracks had propagated

through the pipe thickness and extended for at least 10 inches around the pipe at the weld toe for both specimens.

It quickly became apparent during the course of the experimental work that the galvanized coating made it difficult to detect small cracks. This can be seen in Fig. 36 where the crack front was marked after 265,000 cycles of loading. At that time the small crack sketched in Fig. 36 could not be seen. The galvanized coating did not break and permit the crack to become apparent. Attempts were also made to locate small cracks with a magnetic probe and with an eddy current probe. Neither method was successful. The galvanized coating interfered with both of these methods and it was not possible to detect small cracks.

Since small cracks were not visible because of the galvanized coating, several specimens with no visible indication of cracking had segments cut from the pipe arm and column bases. These segments were cooled in liquid nitrogen and then the pipe segment was broken at the weld toe. This exposed several small cracks including a 0.06 in. deep crack in the pipe arm of specimen V6. Figure 38 shows the fatigue crack surface that was exposed in specimen V6.

Similar small cracks were found at the column base connections of specimens V4 and A6. These are shown in Fig. 39 and 40. Figure 39 shows the cracks found at the base of specimen V4. These cracks were 0.02 to 0.03 in. deep and varied in width along the weld toe. Their length was between 0.2 and 0.4 in.

Figure 30 shows a crack at the column base of specimen A6. This crack was 0.08 in. deep and was 0.35 in. long.

None of the cracks shown in Figs. 38 to 40 had propagated through the zinc coat. The results suggest that the crack must propagate nearly through the pipe thickness before it can be detected if a single crack as shown in Fig. 40 exists. A longer multiple coalesced crack will likely break the galvanized coating before forming a through thickness crack.

7. SUMMARY AND CONCLUSIONS

The results of this series of tests on standard California Department of Transportation Light Pole details has provided information on the behavior and fatigue resistance of the welded details. The following observations can be made from the results of this investigation.

1. The fatigue strength of the fillet welded connections at the arm connection plates and at the column base plates were much lower than anticipated. The original A283 Grade D steel pole specimens with equal leg fillet welds provided a fatigue resistance generally less than Category E'. The A595 Grade A specimens with unequal leg fillet welds provide a fatigue resistance equal to Category E'.
2. All failures occurred from the fillet weld toe on the pipe arm or column. Most specimens had significant cracks at both locations. This was reasonable as the cyclic stress was about the same at both details.
3. The fillet weld inclination for the original A283 Grade D steel specimens was between 45° and 47° for the arm and column. The fillet weld inclination for the A595 Grade A steel specimens was between 27° and 28° . This provided a significant reduction in the stress concentration and improved the fatigue resistance of the light poles.

4. The two supplemental test specimens fabricated from A283 Grade D steel that had unequal leg fillet welds experienced a significant improvement in fatigue resistance. They both failed at the Category E design curve when tested at 6.4 ksi stress range which was a significant improvement. Although both specimens provided slightly less fatigue life than the A595 Grade A steel specimens, the difference is not significant considering the number of specimens that was tested and the scatter in the test data. The improvement in fatigue resistance can be attributed to the decrease in fillet weld inclination angle. This angle was measured to be about 34° for the two supplemental test specimens at the pipe arm where failure occurred.
5. Further research should be carried out to find ways to improve the fatigue resistance of the pipe arm and column base connections. The use of the lowest possible fatigue resistance detail (Category E') indicates that cumulative fatigue damage and eventual cracking is likely. It is recommended that consideration be given to tests with peened or gas tungsten arc remelt weld toe conditions as one possible way to increase fatigue resistance. Alternate details could also be examined for the arm-column connection such as directly welding the arm to the column.

6. This experimental study has also demonstrated that small fatigue cracks are difficult if not impossible to detect at galvanized details. The galvanized coating permits large cracks to form before it breaks and exposes the crack. Hence most of the fatigue life is already exhausted before cracks are likely to be detected.

8. IMPLEMENTATION

CALTRANS' Standard Plans ES-6Q, 6R, and 6S will be revised to allow thin wall steel poles as an alternate to current details on a trial basis. The alternate poles must have a minimum yield strength of 48 ksi and utilize the unequal leg fillet weld provided on the test specimens. The alternate poles are expected to provide modest cost savings. More extensive application of the alternate design is subject to pole performance data and documented savings gained from actual installations.

ACKNOWLEDGMENTS

This study was carried out at the Fritz Engineering Laboratory Lehigh University, Bethlehem, Pennsylvania for the California Department of Transportation and the Federal Highway Administration of the U. S. Department of Transportation.

The authors acknowledge the assistance of many members of the support staff. Messrs. Robert Dales and Raymond Kromer assisted with the experimental work. Mrs. Dorothy Fielding typed the manuscript, Mr. Richard Sopko provided the photographs and Mrs. Sharon Balogh drafted the figures. Special thanks are also due Mr. William Frank who was responsible for completing the tests after Dr. Miki returned to Japan.

REFERENCES

1. AASHTO
STANDARD SPECIFICATIONS FOR HIGHWAY BRIDGES,
Twelfth Edition, 1977.
2. Baxter, D. E. and Modlen, G. F.
SOME FACTORS AFFECTING THE FATIGUE STRENGTH OF FILLET WELDS,
British Welding Journal, Vol. 13, No. 4, 1966, pp 184-188
3. Frank, K. H.
THE FATIGUE STRENGTH OF FILLET WELDED CONNECTIONS,
Ph.D. Dissertation, Lehigh University, Bethlehem, PA.
October 1971.
4. Fisher, J. W., Albrecht, P. A., Yen, B. T., Klingerman, D. J.
and McNamee, B. M.
FATIGUE STRENGTH OF STEEL BEAMS WITH WELDED STIFFENERS AND
ATTACHMENTS,
NCHRP Report 147, Transportation Research Board, 1974.
5. Fisher, J. W., Hausammann, H., Sullivan, M. D. and Pense,
A. W.
DETECTION AND REPAIR OF FATIGUE DAMAGE IN WELDED HIGHWAY
BRIDGES, NCHRP Report 206, Transportation Research Board, 1979.

TABLE 1 STRAIN MEASUREMENTS

SPECIMEN V4 STATIC LOAD TEST

(micro-inch)

<u>Load</u> <u>(kips)</u>	<u>Gage 5</u>	<u>Gage 6</u>	<u>Gage 7</u>	<u>Gage 8</u>	<u>Gage 9</u>	<u>Gage 10</u>	<u>Gage 11</u>	<u>Gage 12</u>
1	150	125	- 15	- 139	- 167	- 125	0	135
2	310	265	- 30	- 284	- 340	- 255	0	280
3	485	410	- 60	- 444	- 535	- 400	0	425
4.1	665	560	- 75	- 614	- 730	- 545	0	580
1.2	180	150	- 10	- 170	- 200	- 145	0	160

TABLE 2 SUMMARY OF FATIGUE TEST RESULTS

Spec. No.	Load [†] (kips)	Nominal Stress Range*		Measured Strain x 10 ⁻⁶				Deflection x 10 ⁻³ (in.)	Fatigue Life	Failure Location and Crack Size**	
		Sec. I	Sec. II	Sec. I (Arm)		Sec. II (Base)				Arm	Base
				Gage 2	Gage 4	Gage 1	Gage 3				
A1	1.5 ~ 7.1	18.8	18.9	120 ~ 615	-125 ~ -720	---	-110 ~ -640	260 ~ 1600	36,100	Failure	10 in.
A2	1.5 ~ 5.2	12.4	12.5	100 ~ 460	-140 ~ -550	95 ~ 490	-130 ~ -530	250 ~ 1115	117,800	Failure	--
A3	1.5 ~ 3.4	6.4	6.4	125 ~ 310	-150 ~ -330	145 ~ 330	-140 ~ -340	262 ~ 650	1,892,400	Failure	4 in.
A4	1.5 ~ 5.2	12.4	12.5	140 ~ 485	-165 ~ -535	155 ~ 535	-145 ~ -570	376 ~ 1096	174,200	Failure	11 in.
A5	1.5 ~ 3.4	6.4	6.4	125 ~ 300	-165 ~ -370	140 ~ 340	-155 ~ -345	340 ~ 750	1,208,700	Failure	0.25 in x 6 in.
A6	1.5 ~ 3.4	6.4	6.4	149 ~ 341	-174 ~ -385	128 ~ 317	-175 ~ -386	274 ~ 660	1,472,900	Failure	0.08 in. x 0.35 in.
A7	1.5 ~ 3.4	6.4	6.4	147 ~ 337	-160 ~ -370	160 ~ 367	-155 ~ -352	277 ~ 667	3,751,600	Failure	--
A8	1.5 ~ 3.4	6.4	6.4	133 ~ 328	-148 ~ -358	153 ~ 372	-147 ~ -354	294 ~ 714	3,573,400	Failure	
V1	1.2 ~ 5.6	18.9	19.0	140 ~ 680	-160 ~ -755	180 ~ 850	-160 ~ -745	260 ~ 1360	87,000	Failure	6 in.
V2	1.2 ~ 4.1	12.4	12.6	185 ~ 615	-145 ~ -545	170 ~ 550	-145 ~ -580	283 ~ 1000	317,500	Failure	--
V3	1.2 ~ 2.7	6.4	6.5	160 ~ 350	-145 ~ -355	175 ~ 365	-160 ~ -360	292 ~ 670	5,244,000	5.5 in.	Failure
V4	1.2 ~ 4.1	12.4	12.6	130 ~ 490	---	180 ~ 635	-150 ~ -600	286 ~ 1042	198,100	Failure	0.06 in. x 3 in.
V5	1.2 ~ 2.7	6.4	6.5	140 ~ 335	-155 ~ -360	170 ~ 390	-175 ~ -405	288 ~ 660	5,186,500	--	Failure
V6	1.2 ~ 2.7	6.4	6.5	138 ~ 317	-159 ~ -371	169 ~ 393	-164 ~ -382	297 ~ 675	8,832,300	Small Crack	---

* Minimum Stress = 5 ksi

**Crack Size depth and length at section that did not fail; a dash indicates that no crack was found

†Shows minimum and maximum load.

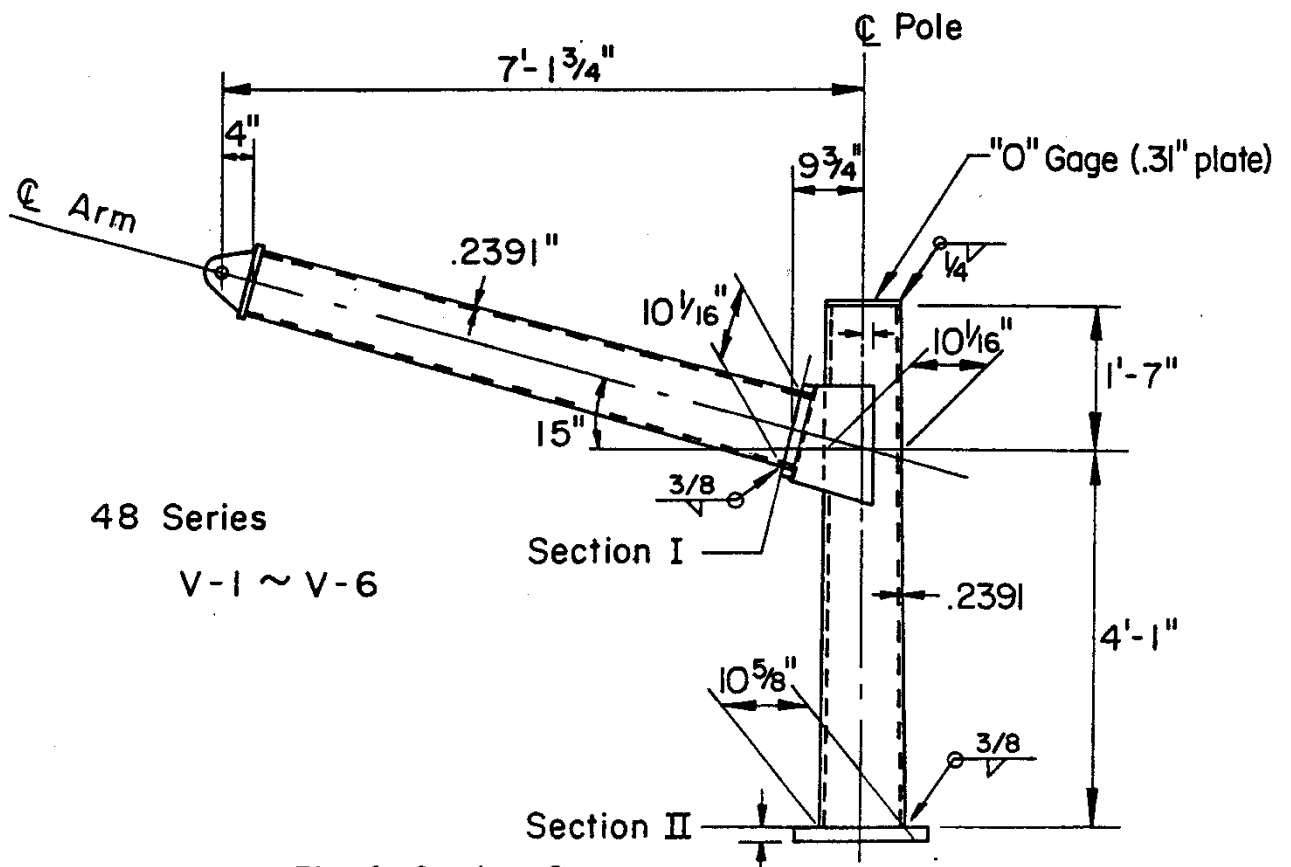
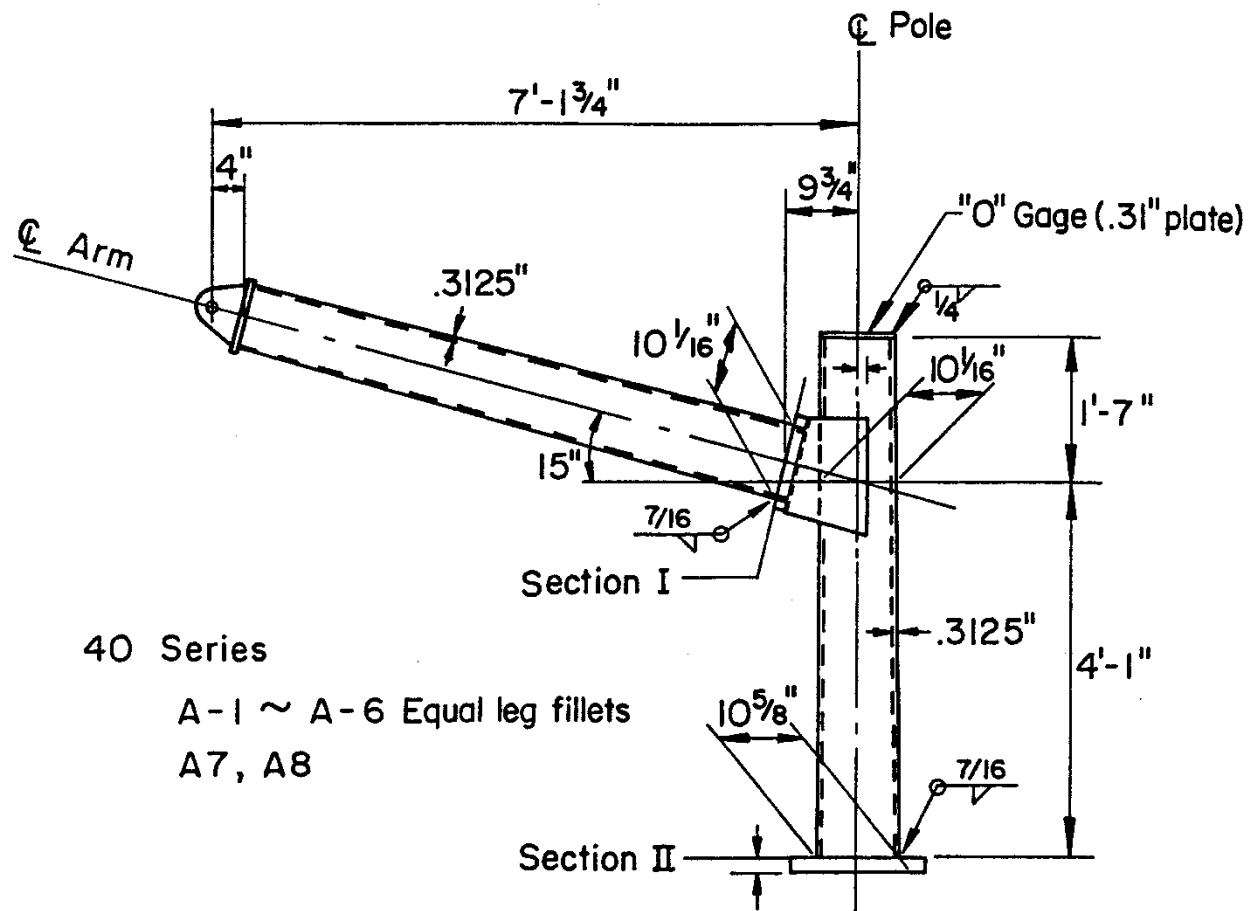
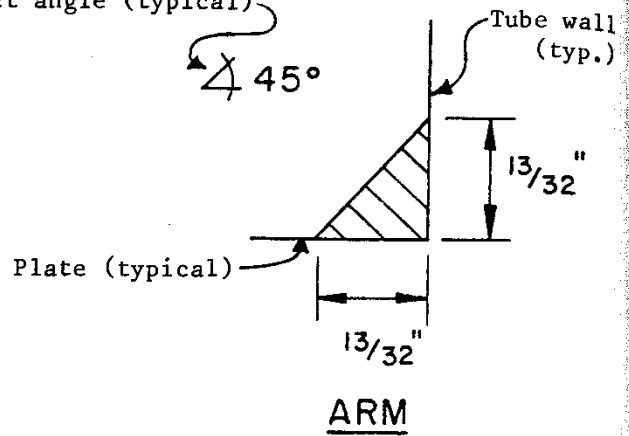
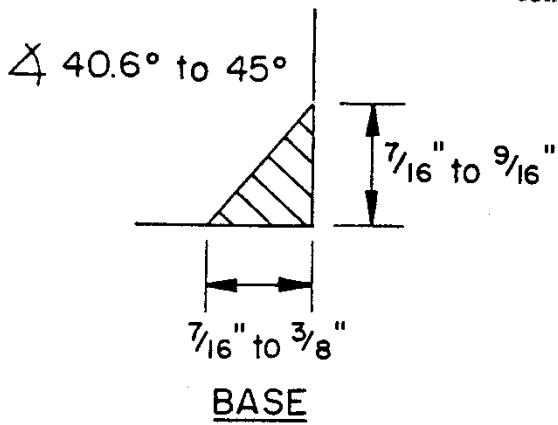


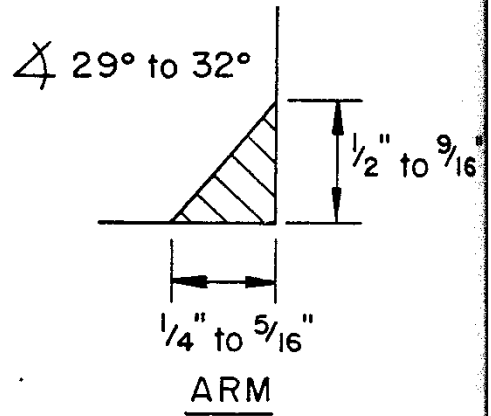
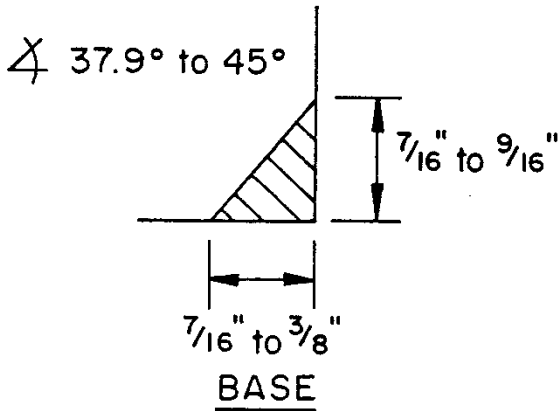
Fig. 1 Specimen Geometry

Specimens A1 to A6

Weld-to-pole
Contact angle (typical)



Specimens A7 & A8



Specimens V1 to V6

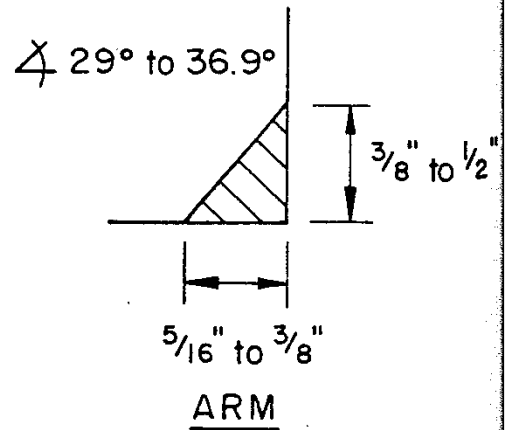
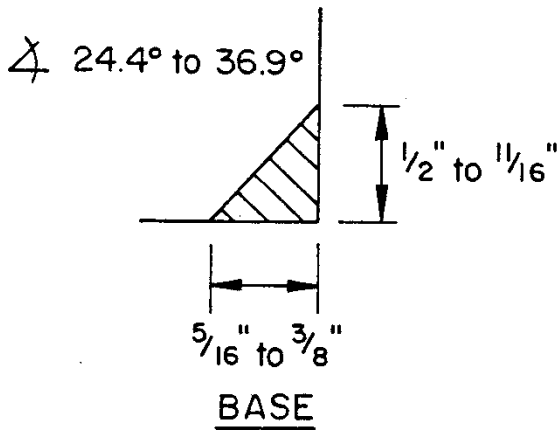
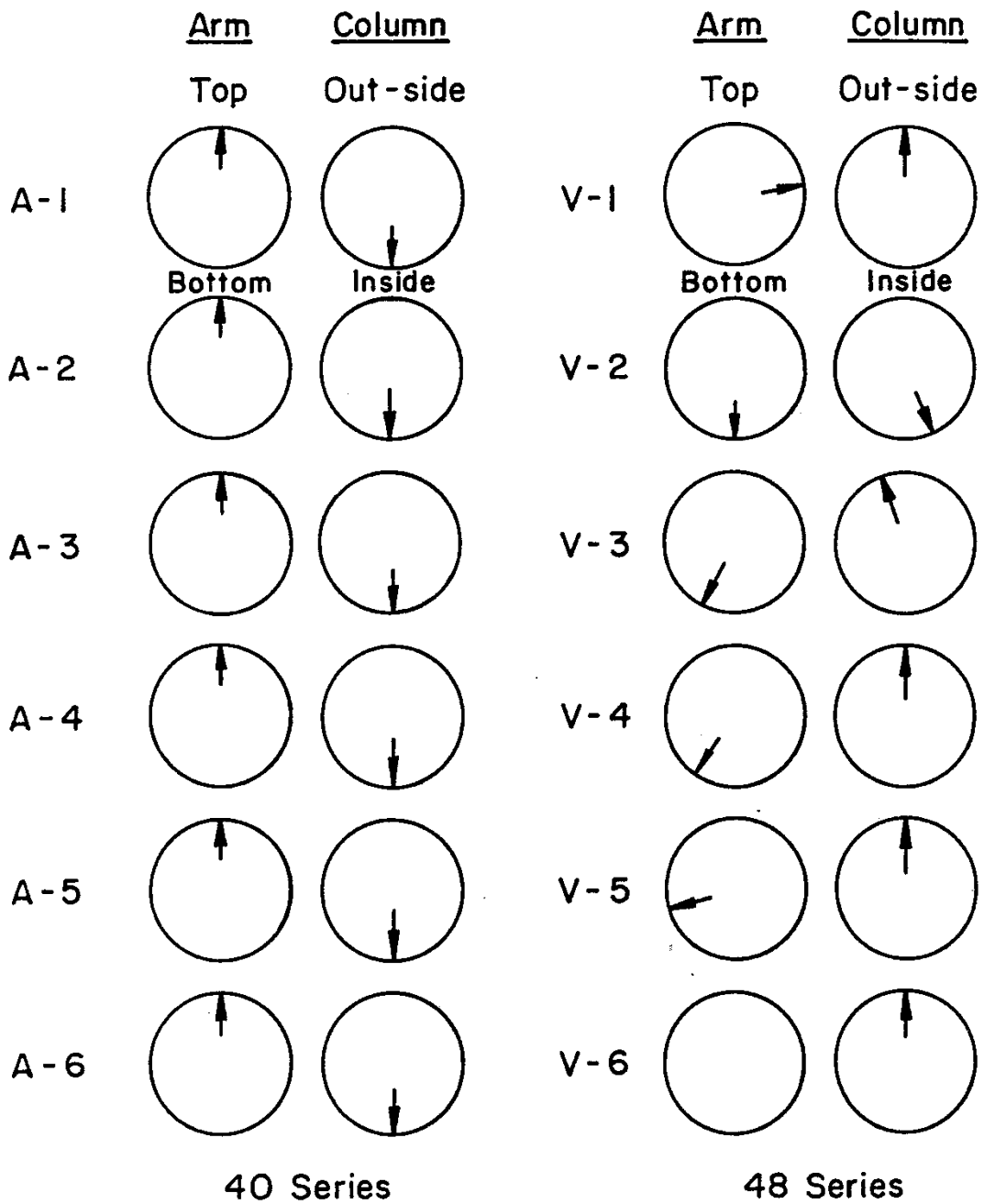
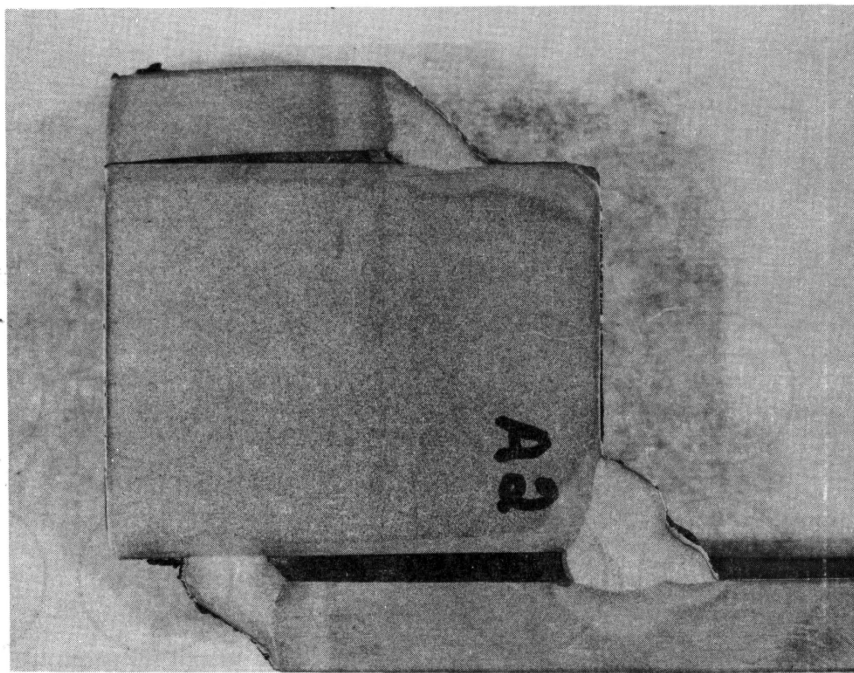


Fig. 1b Summary of Weld Details

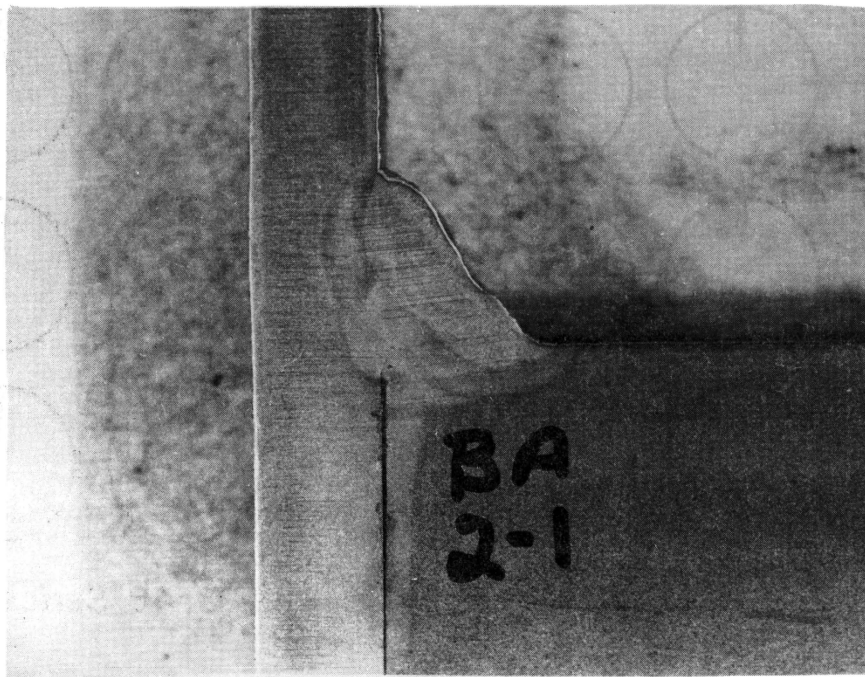


↑ Seam Welding

Fig. 2 Location of Seam Welds on Pipe Arm and Column

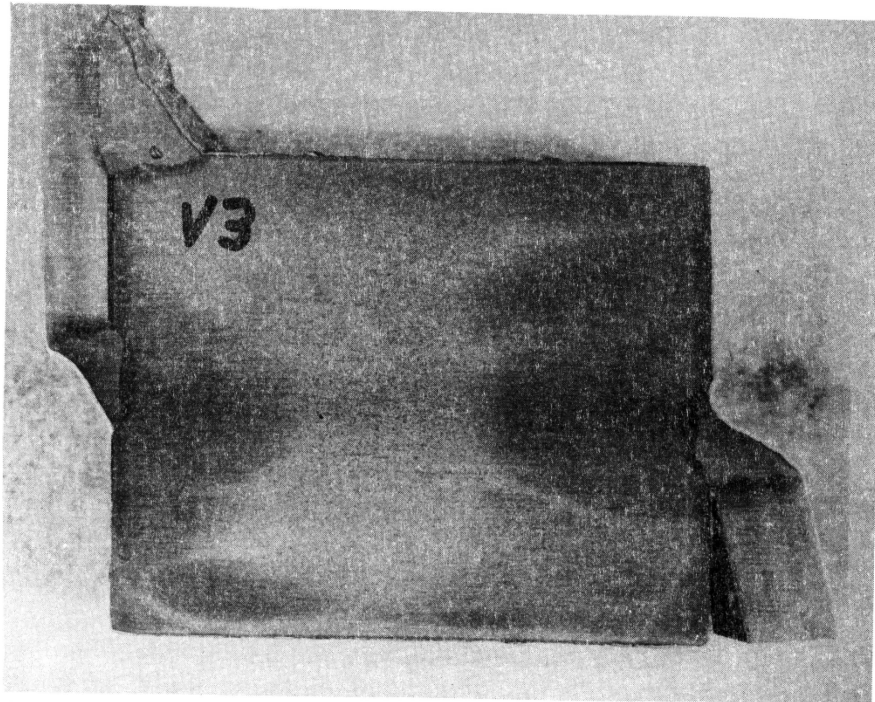


(a) Fillet Weld Profiles for Pipe Arm - Specimen A2

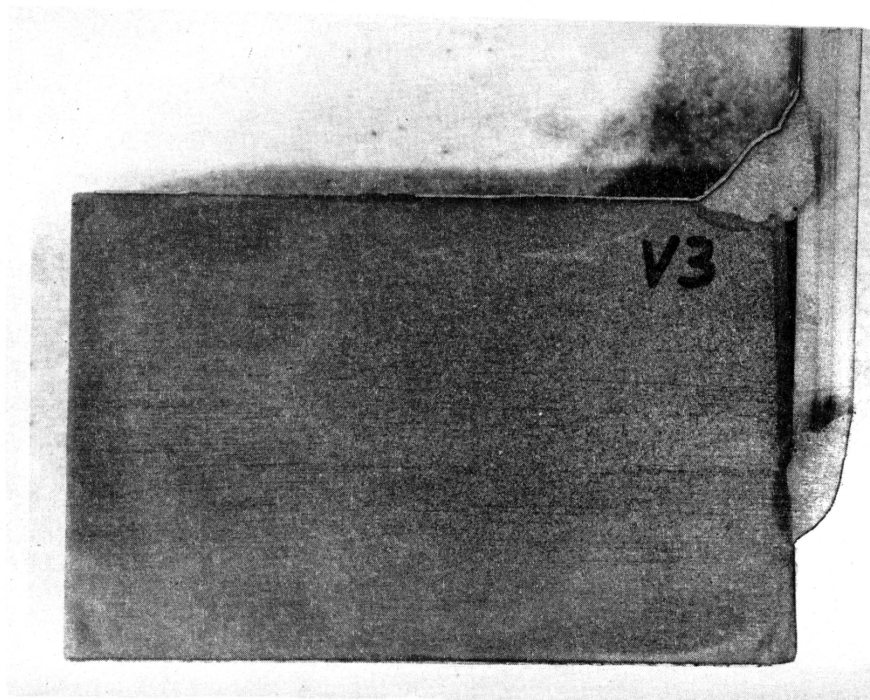


(b) Fillet Weld Profile at Column Base - Specimen A2

Fig. 3 Typical Fillet Weld Profiles for Pipe Arm and Column Base of A Series Specimens (A1 to A6)

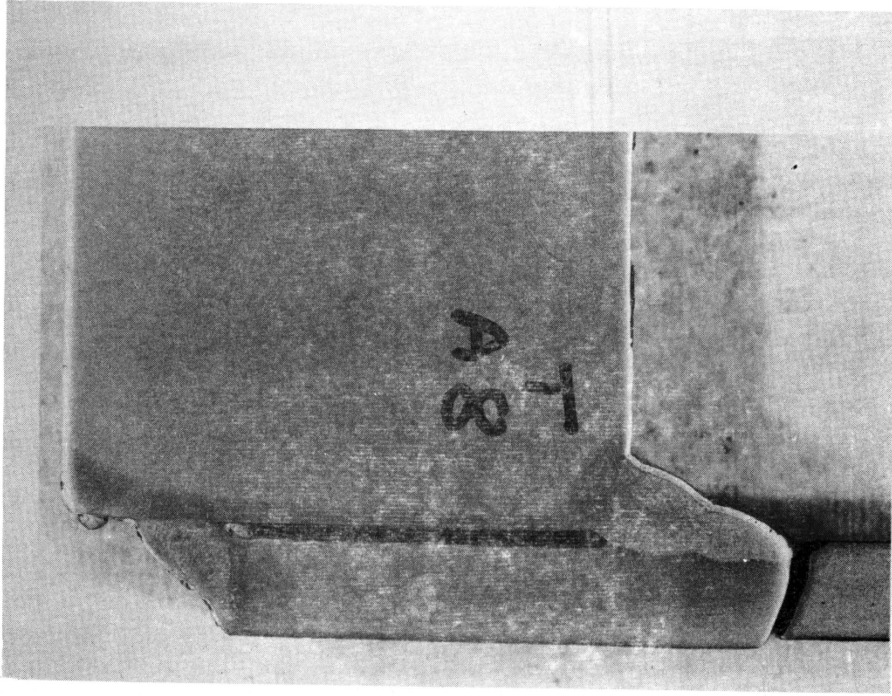


(a) Fillet Weld Profiles for Pipe Arm - Specimen V3

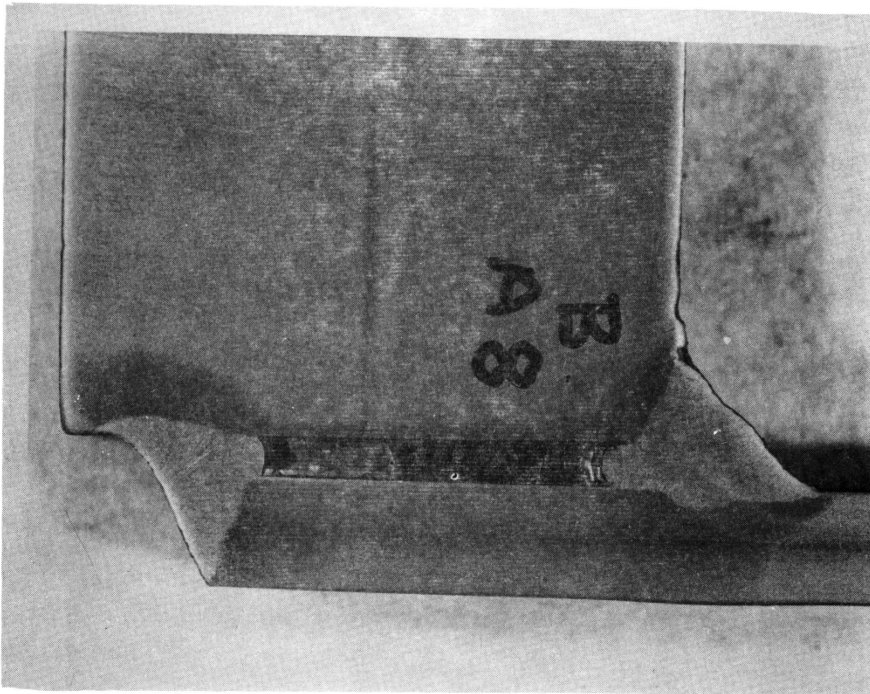


(b) Fillet Weld Profiles at Column Base - Specimen V3

Fig. 4 Typical Fillet Weld Profiles for Pipe Arm and Column Base of V Series Specimens



(a) Fillet Weld Profiles for Pipe Arm - Specimen A8



(b) Fillet Weld Profiles for Column Base - Specimen A8

Fig. 5 Typical Fillet Weld Profiles for Pipe Arm and Column Base of Specimens A7 and A8

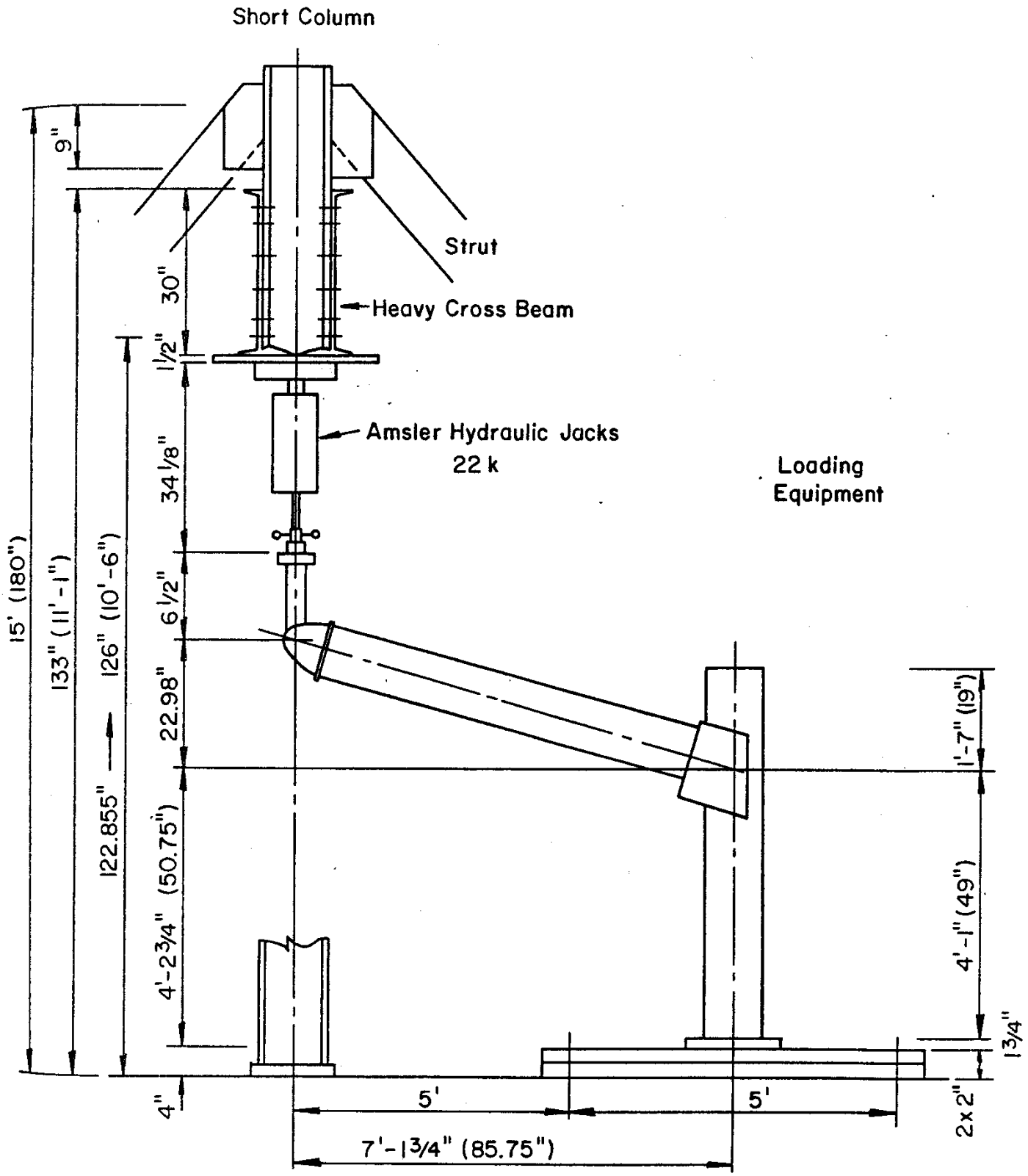


Fig. 6 Test Set-Up

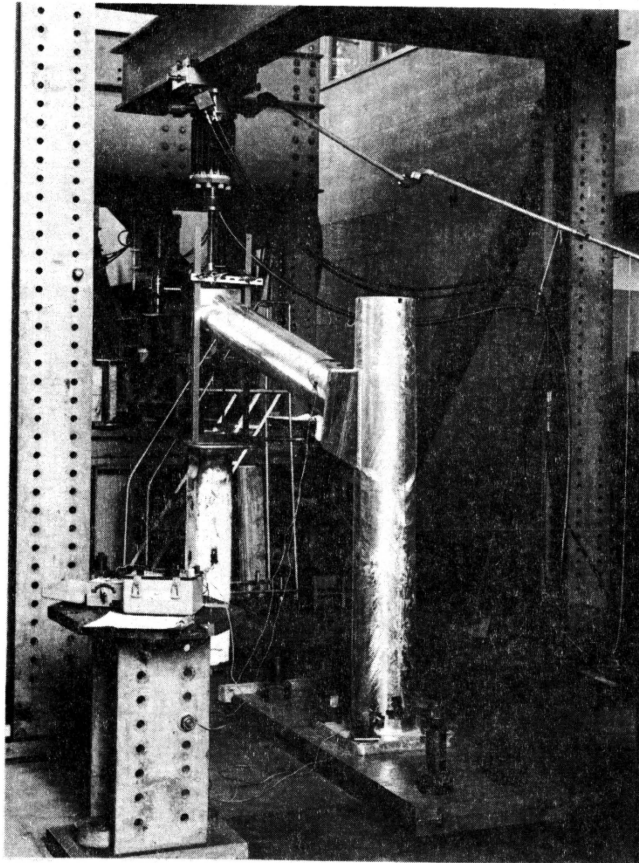


Fig. 7 Testing Set-Up

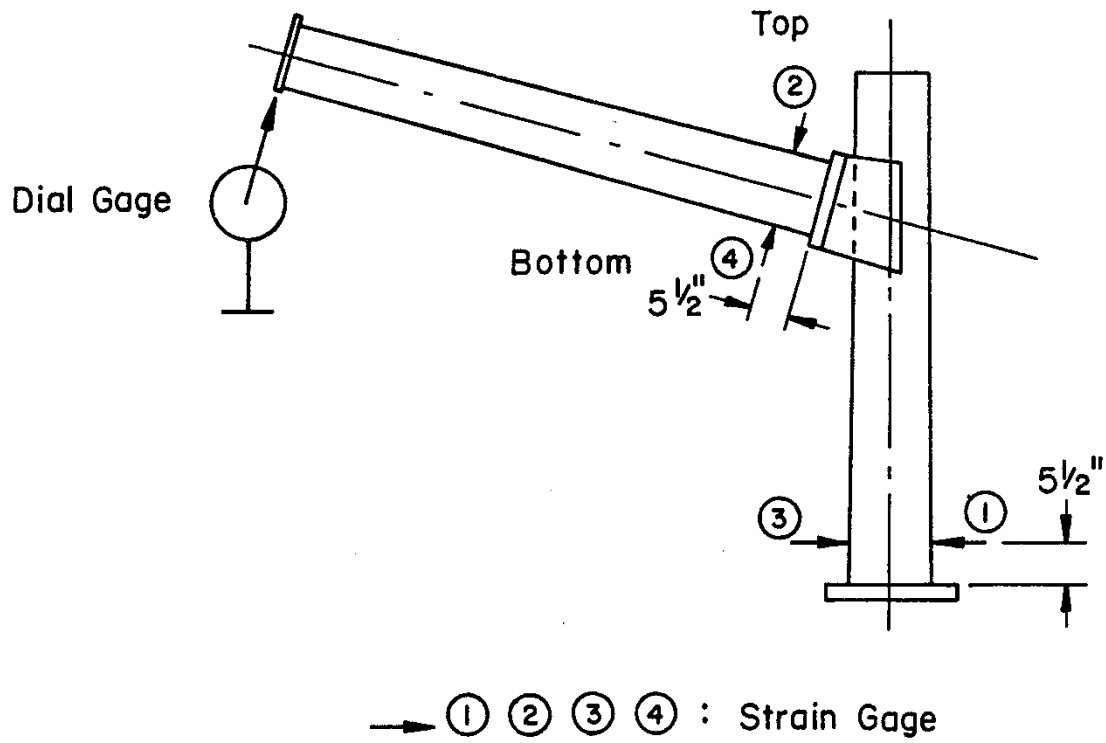


Fig. 8 Location of Strain Gage and Dial Gages

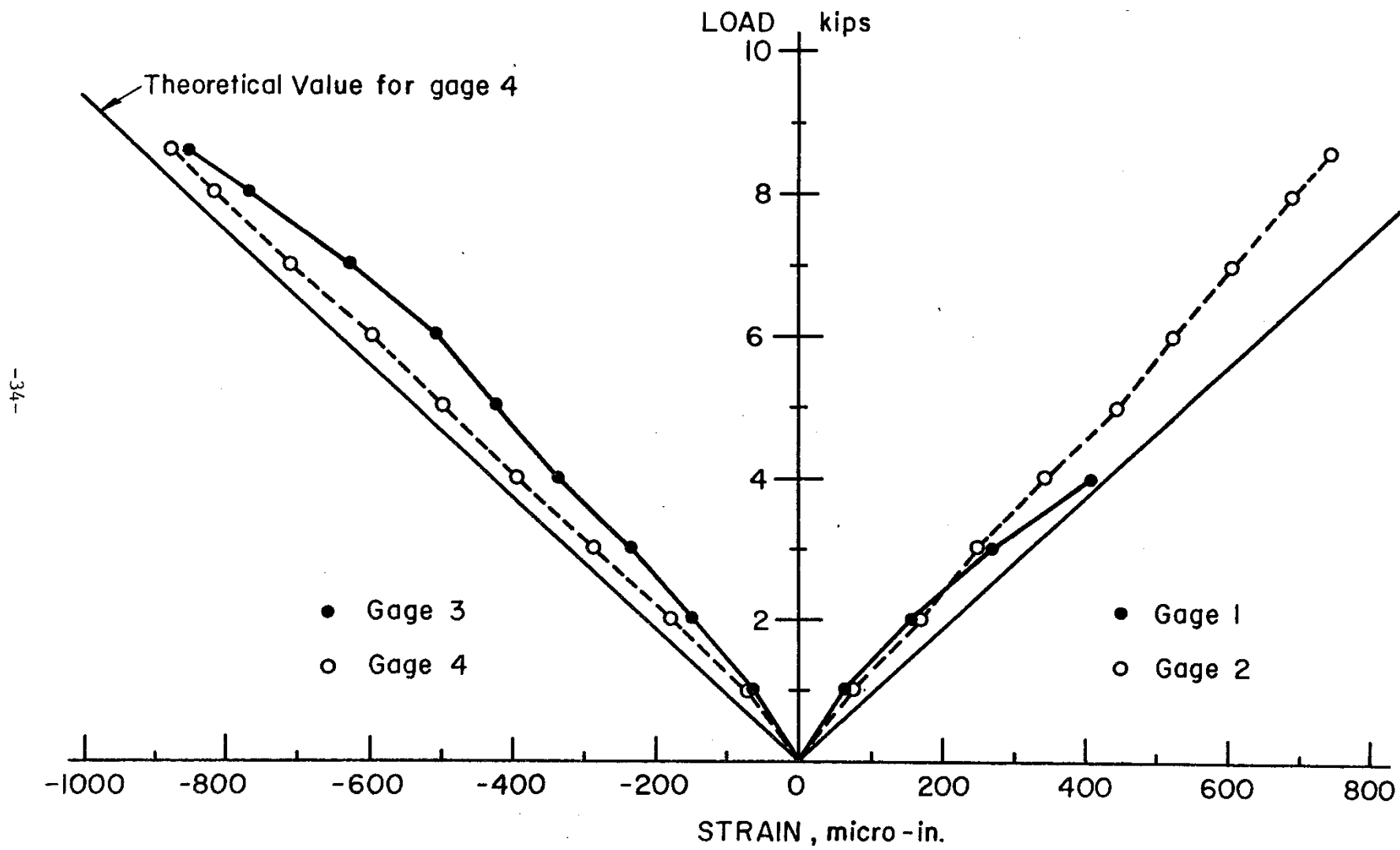


Fig. 9 Measured Strain versus Load for Specimen A1

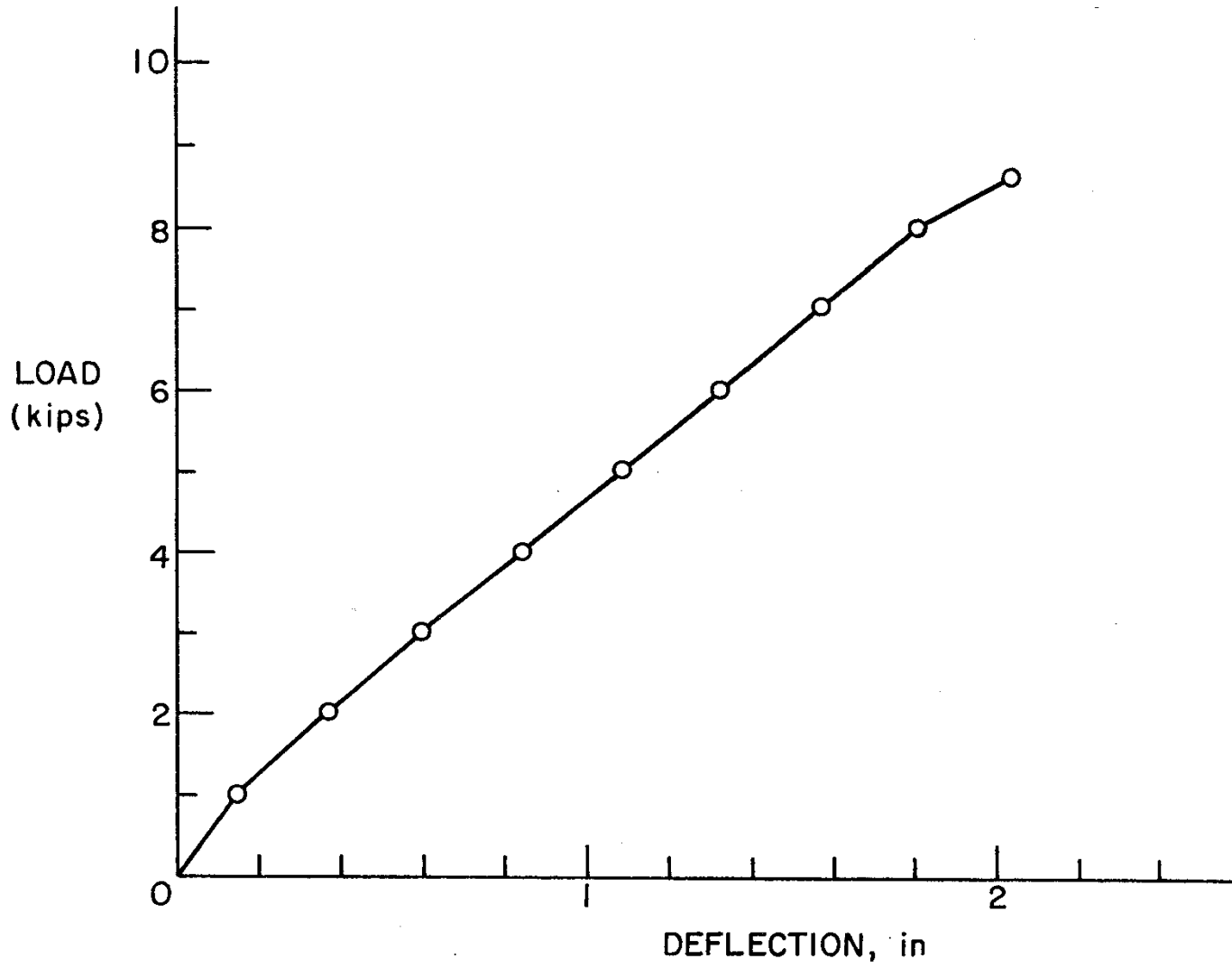


Fig. 10 Measured Load Deflection Behavior of Specimen A1

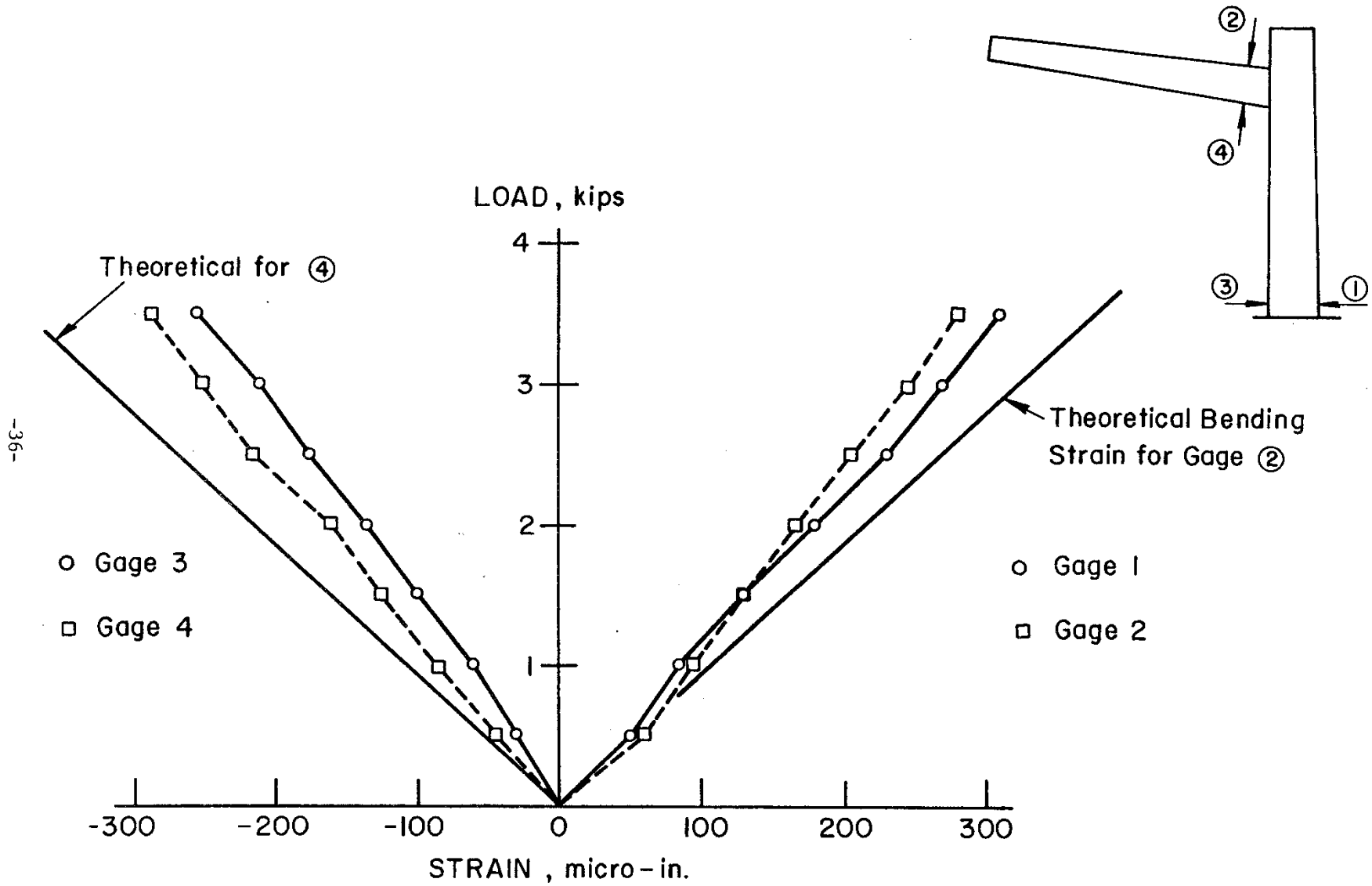


Fig. 11 Comparison of Measured Strain with Predicted Strain - Specimen A1

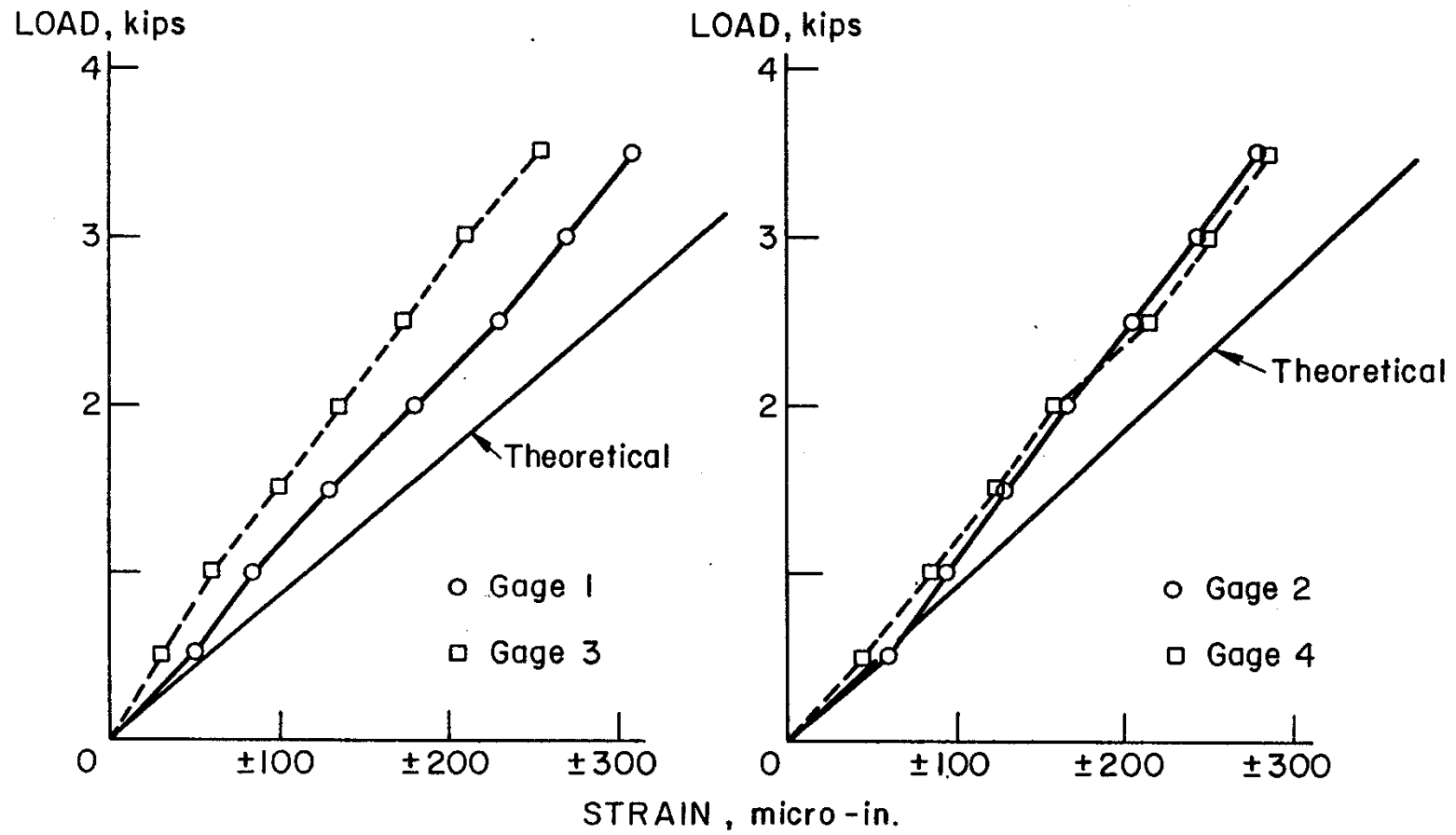


Fig. 12 Comparison of Measured Strain in Pipe and Column with Theoretical Strain - Specimen A1

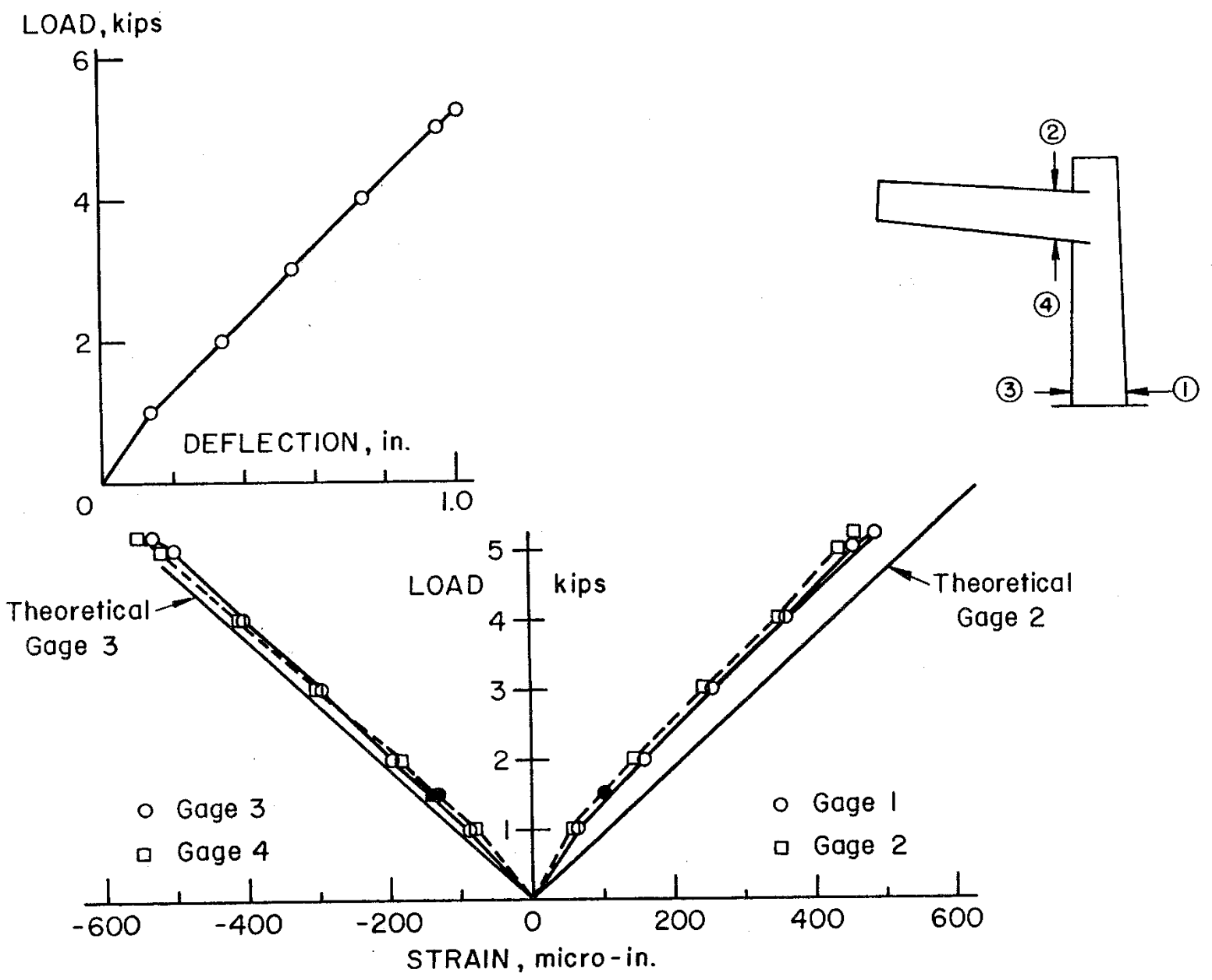


Fig. 13 Load-Deflection and Load-Strain Behavior of Specimen A2

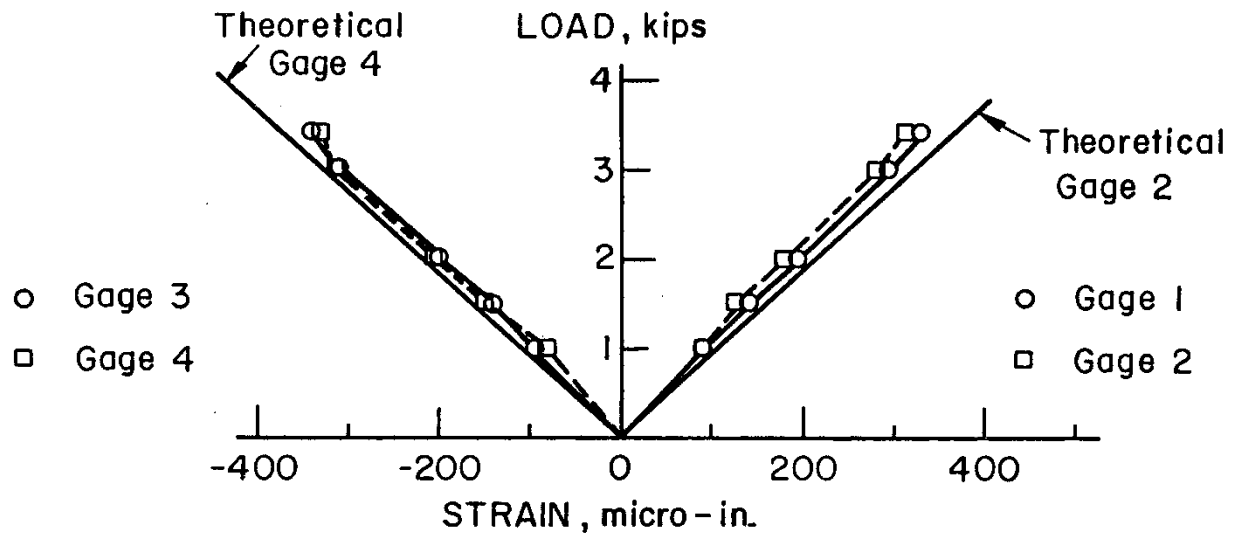
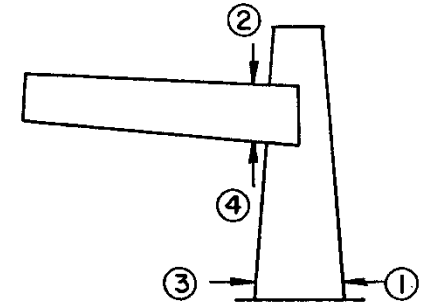
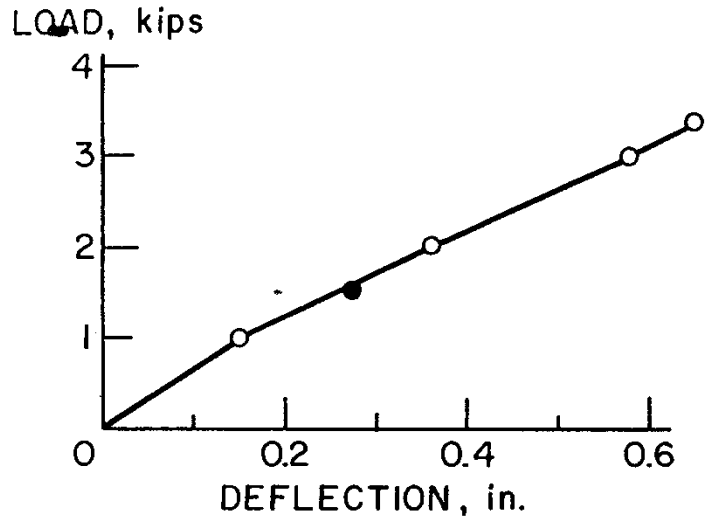


Fig. 14 Load-Deflection and Load-Strain Behavior of Specimen A3

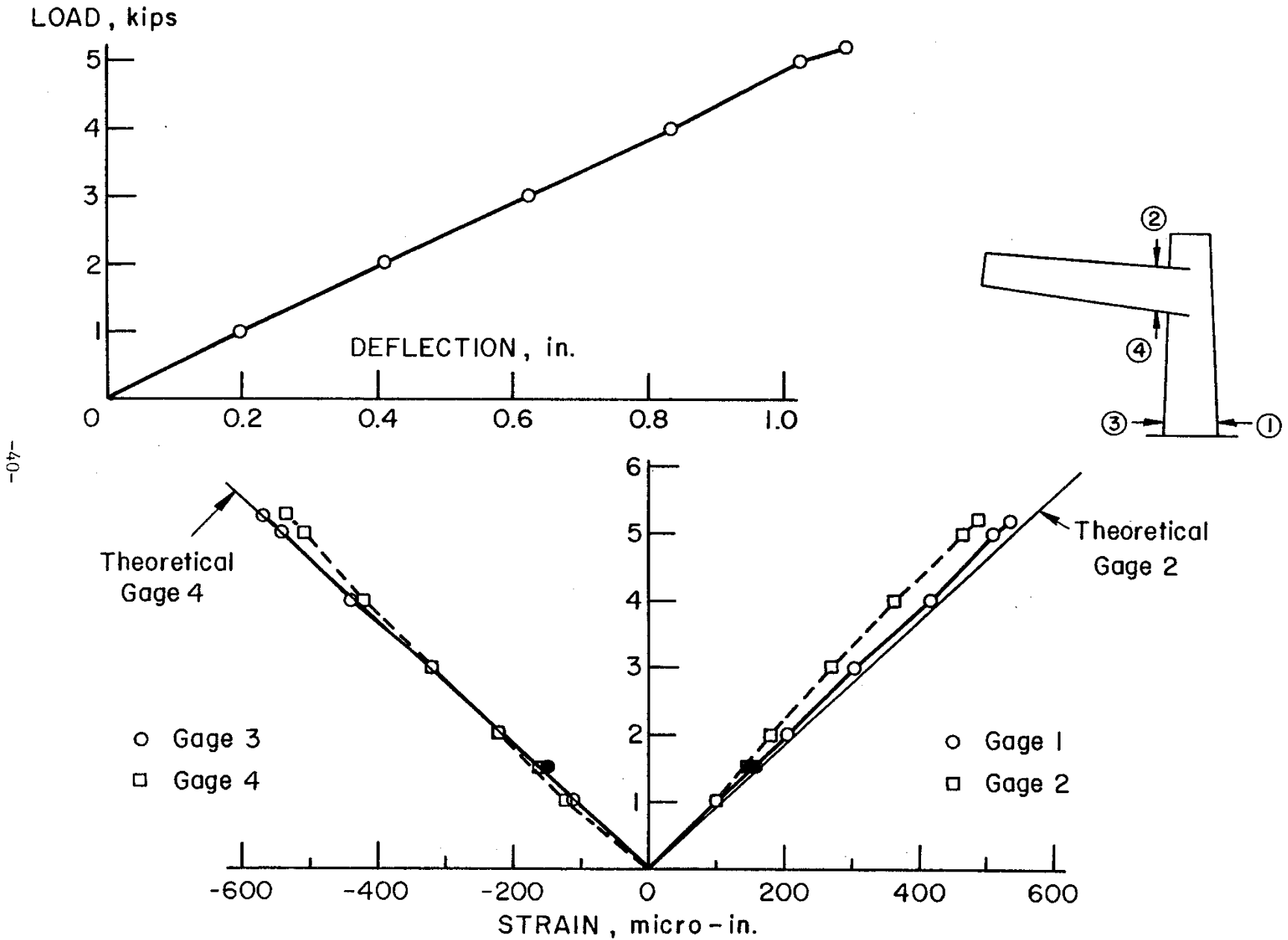
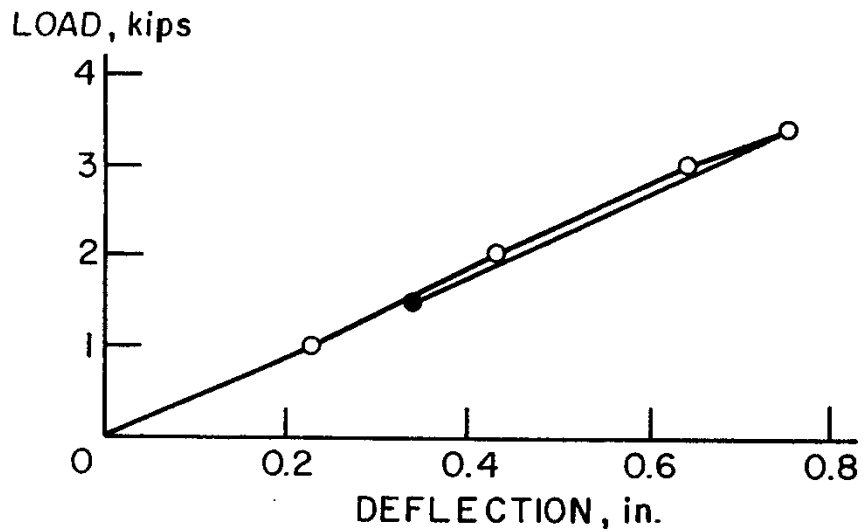


Fig. 15 Load-Deflection and Load-Strain Behavior of Specimen A4



-47-

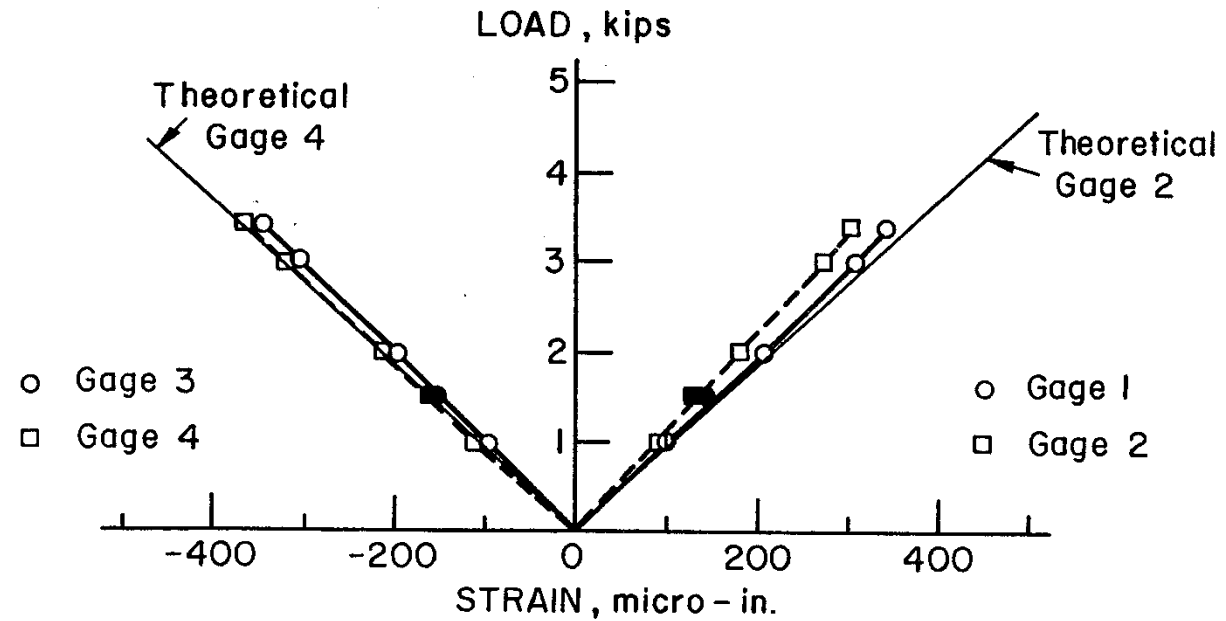
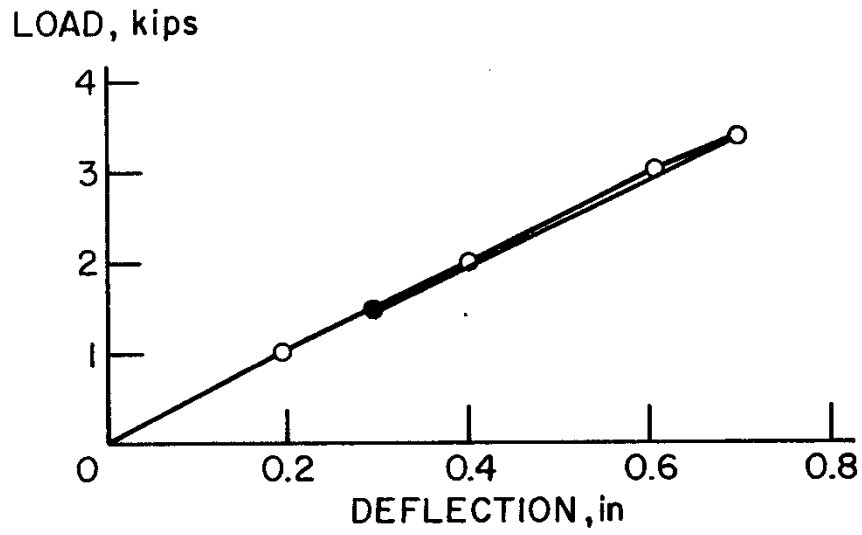


Fig. 16 · Load-Deflection and Load-Strain Relationships for Specimen A5



-42-

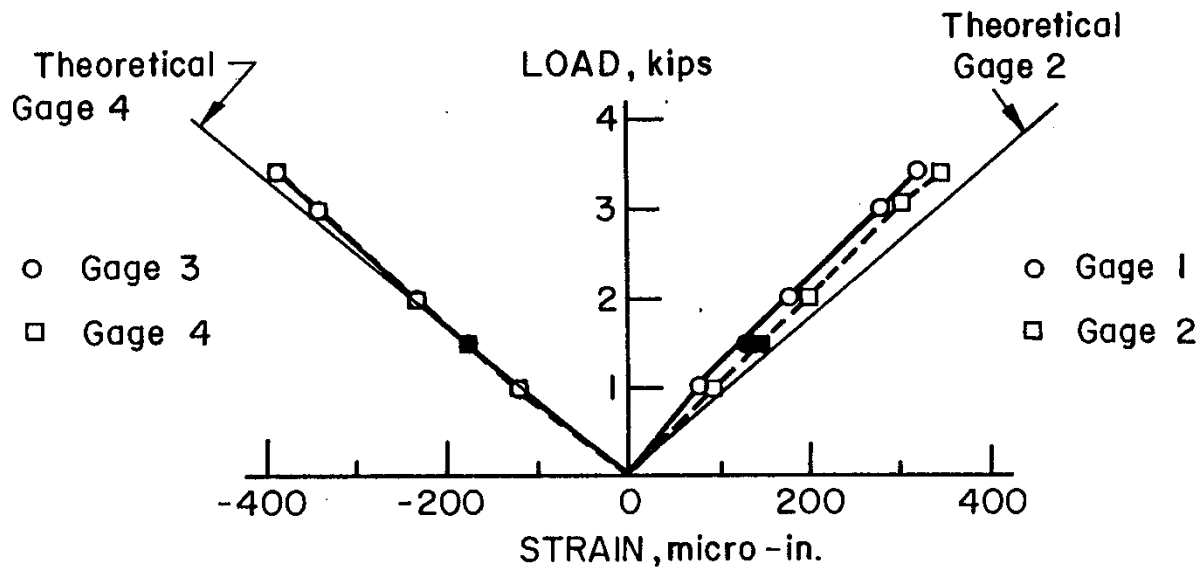
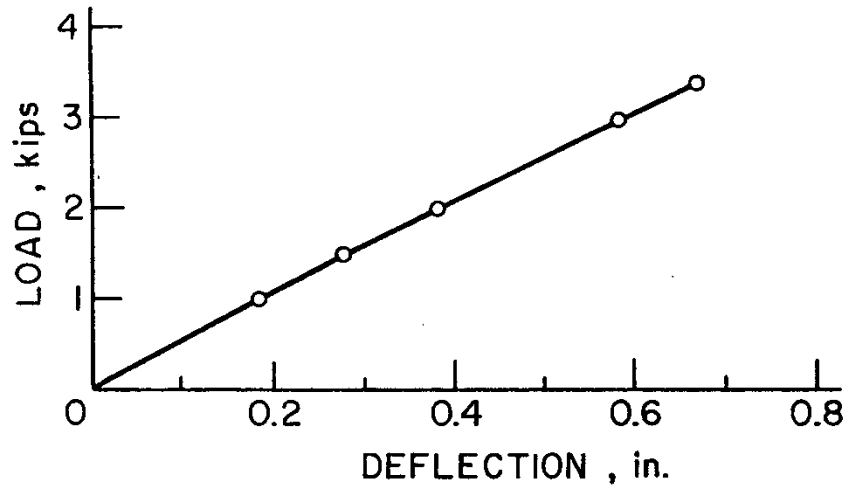


Fig. 17 Load-Deflection and Load-Strain Relationships for Specimen A6



-43-

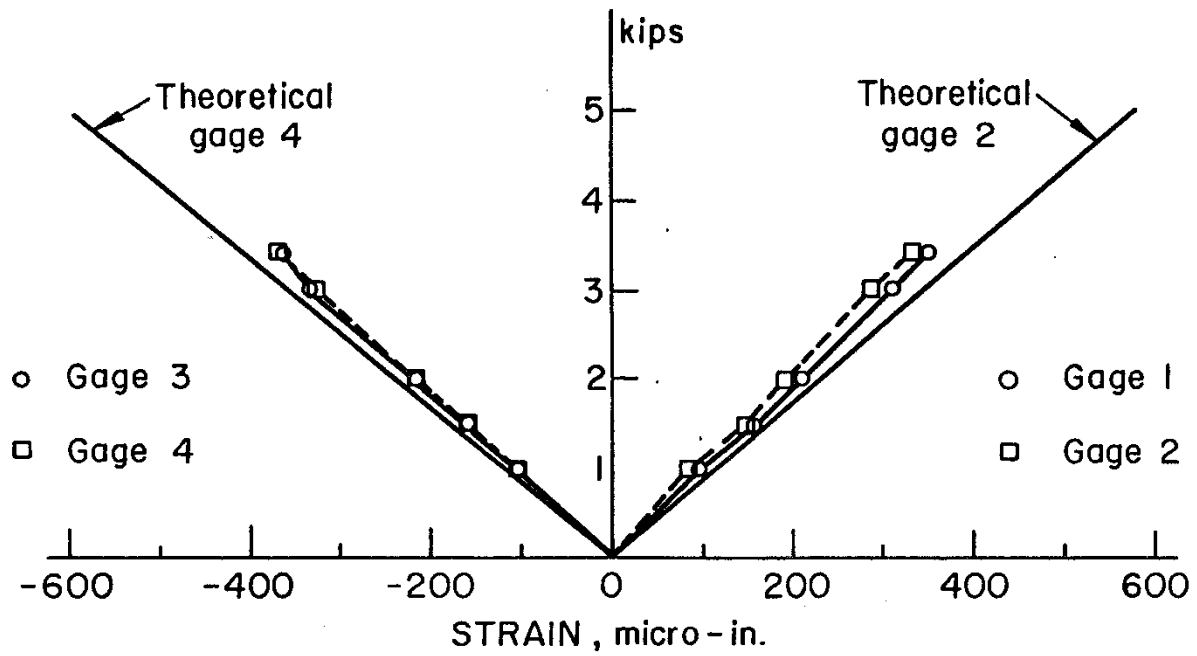
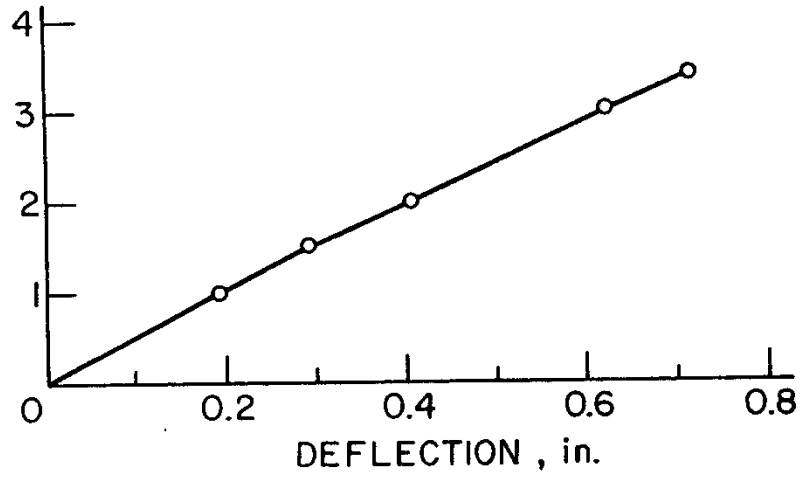


Fig. 18 Load-Deflection and Load-Strain Relationships for Specimen A7



-44-

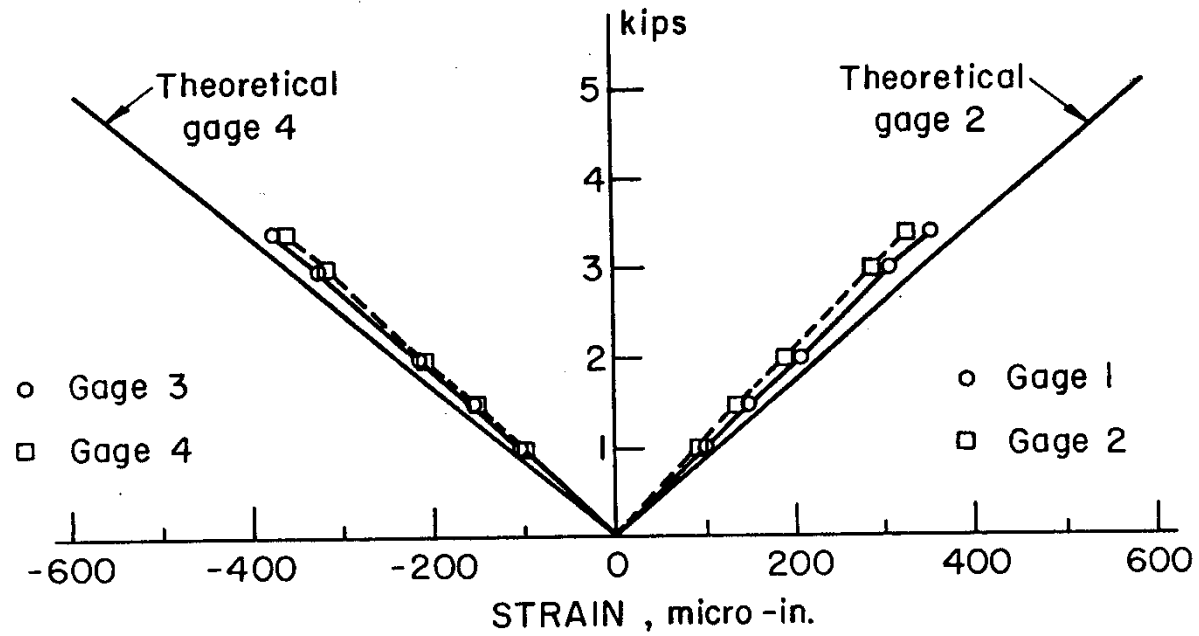


Fig. 19 Load-Deflection and Load-Strain Relationships for Specimen A8

7-45-

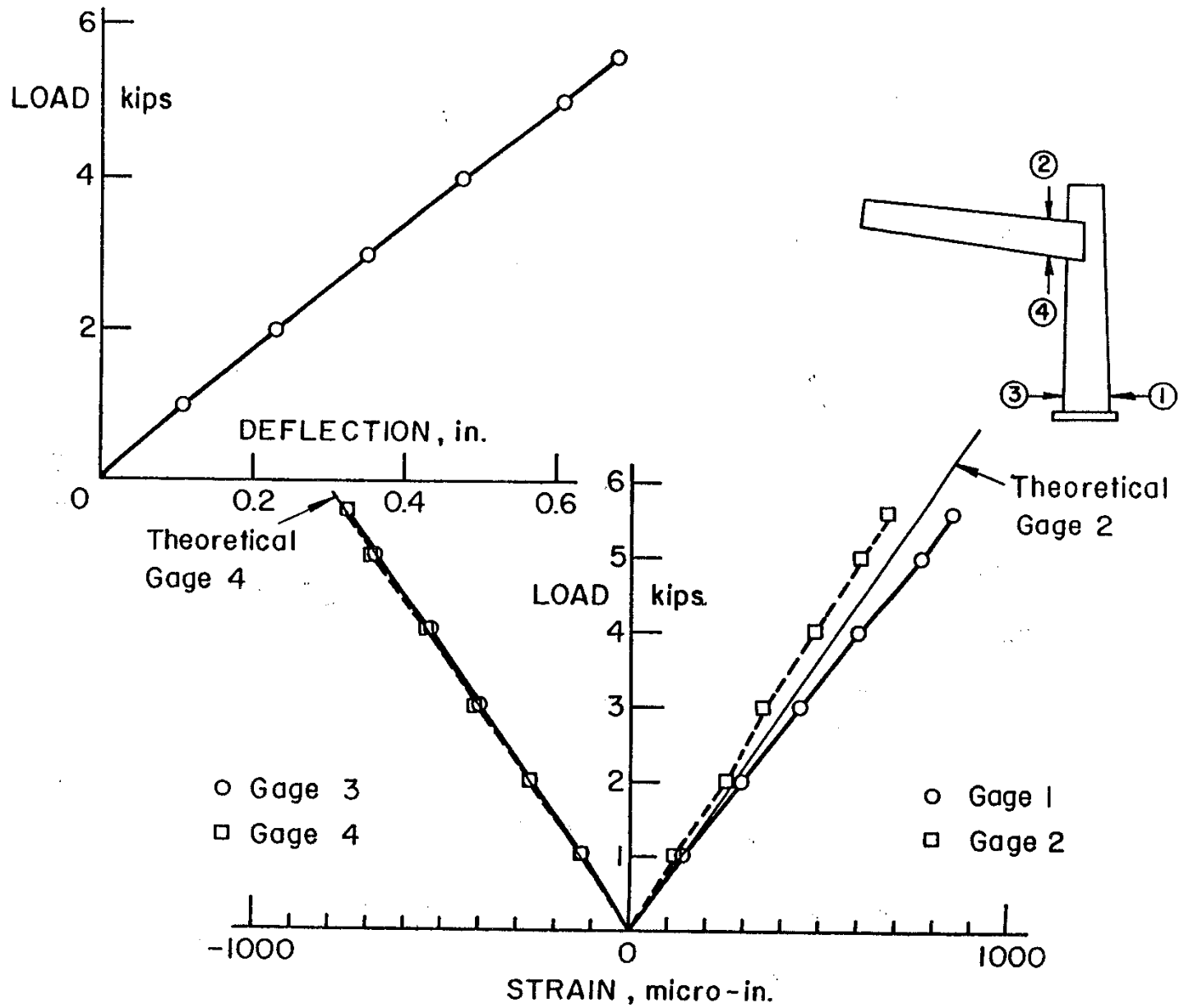
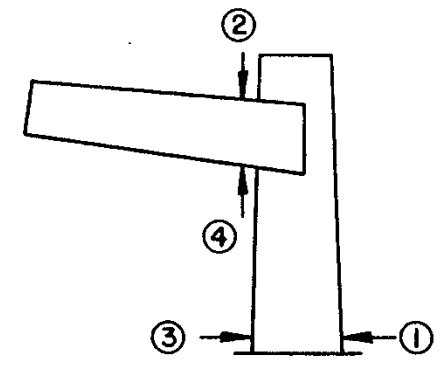
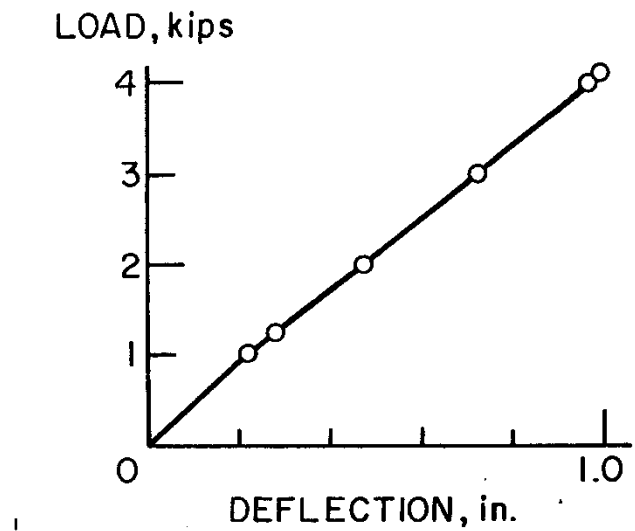


Fig. 20 Load-Deflection and Load-Strain Behavior of Specimen V1



-46-

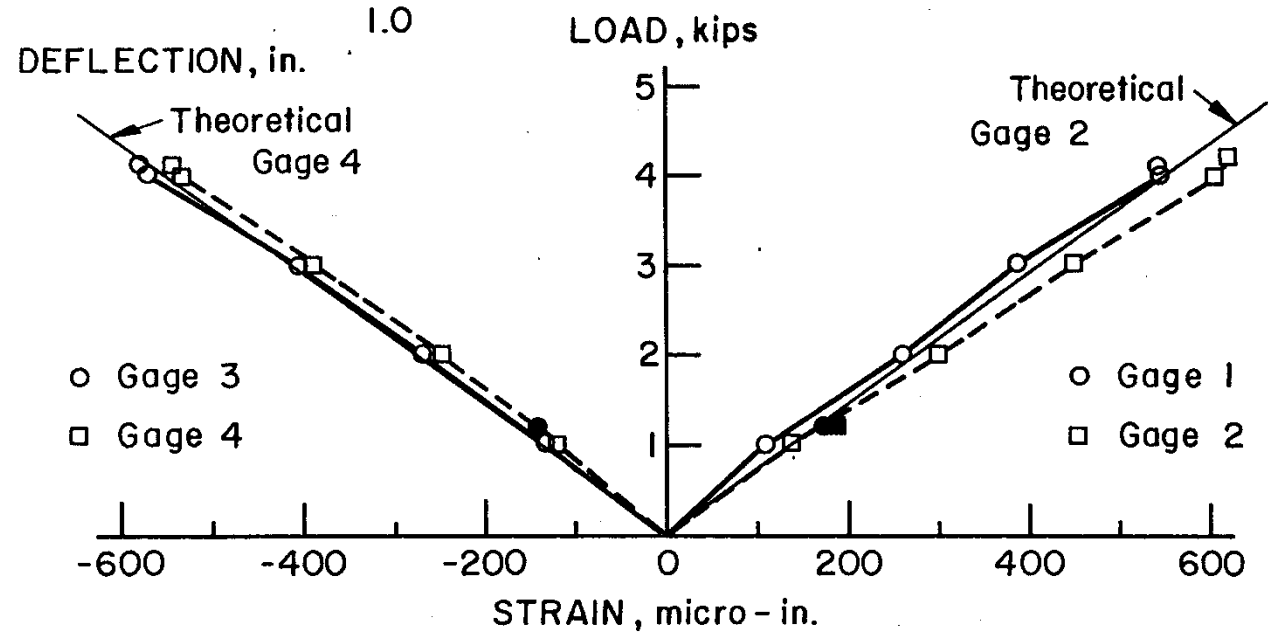


Fig. 21 Load-Deflection and Load-Strain Response of Specimen V2

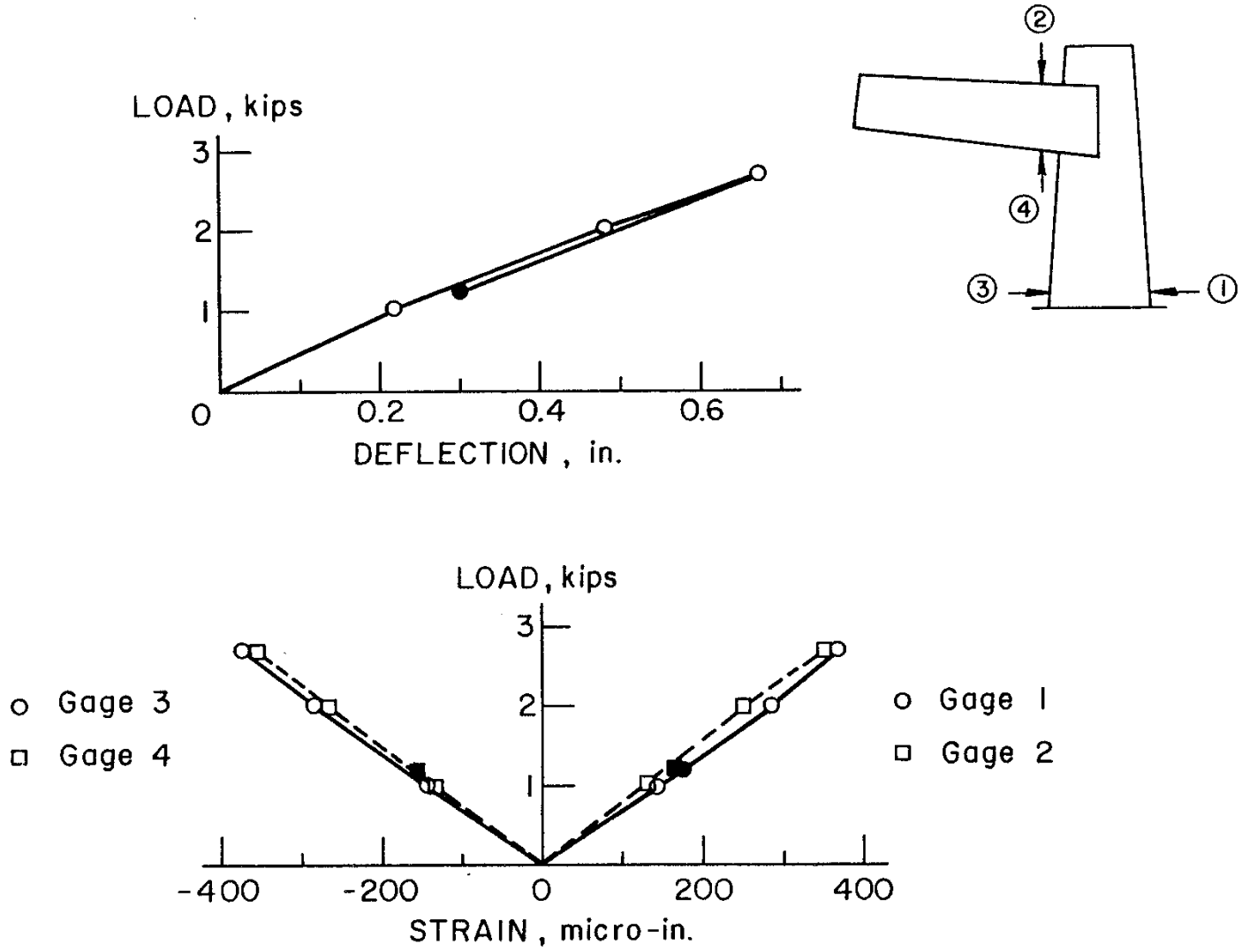
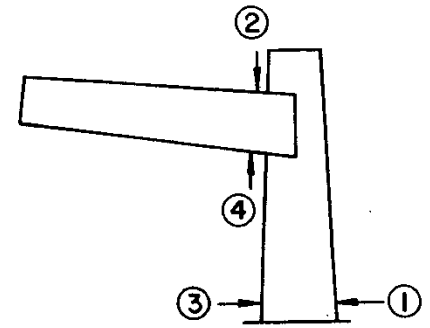
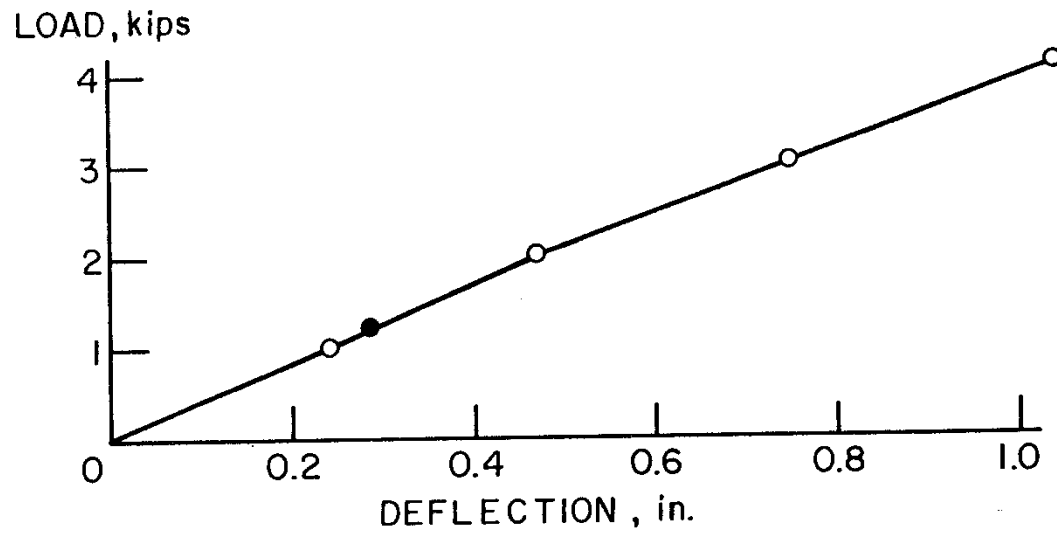


Fig. 22 Load-Deflection and Load-Strain Response of Specimen V3



-48-

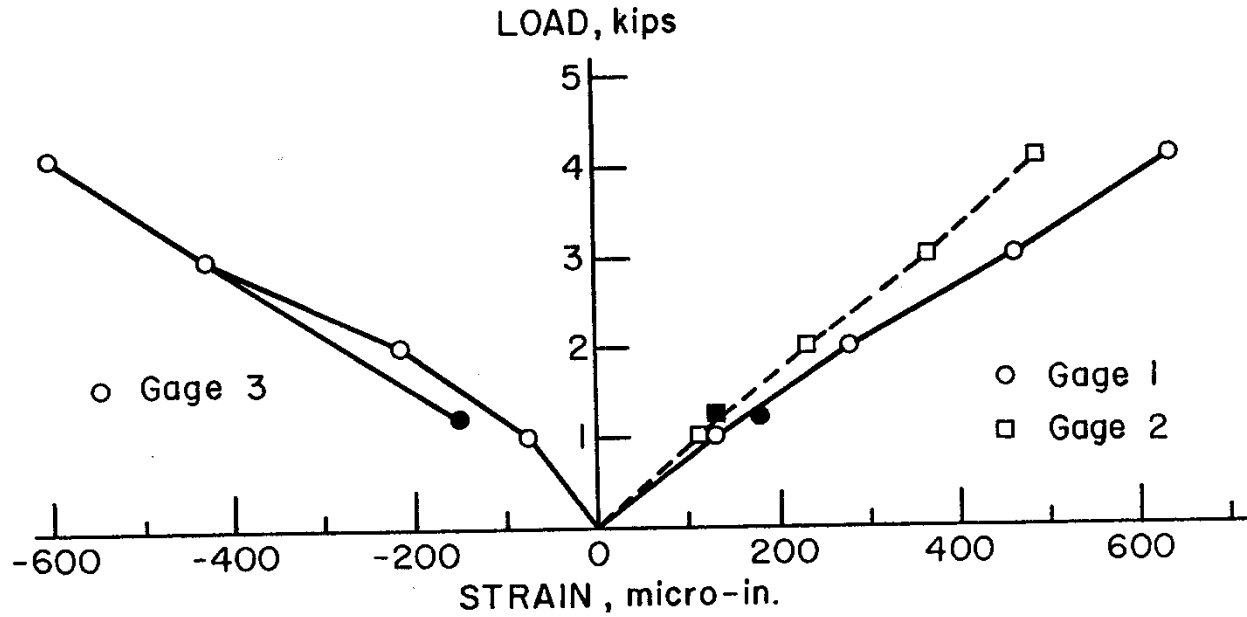
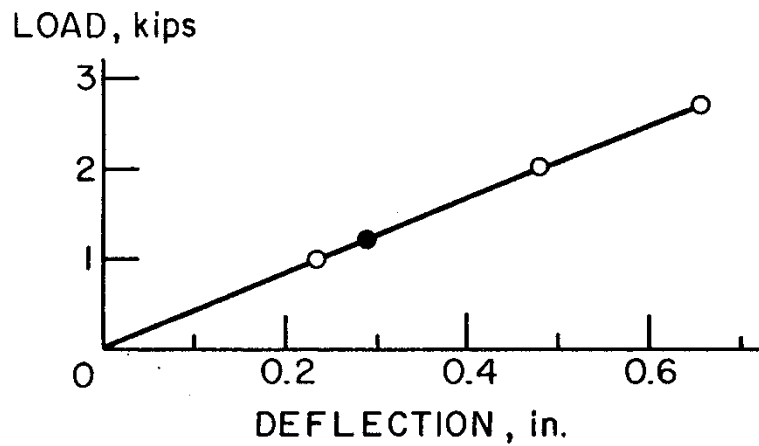


Fig. 23 Load-Deflection and Load-Strain Behavior of Specimen V4



-49-

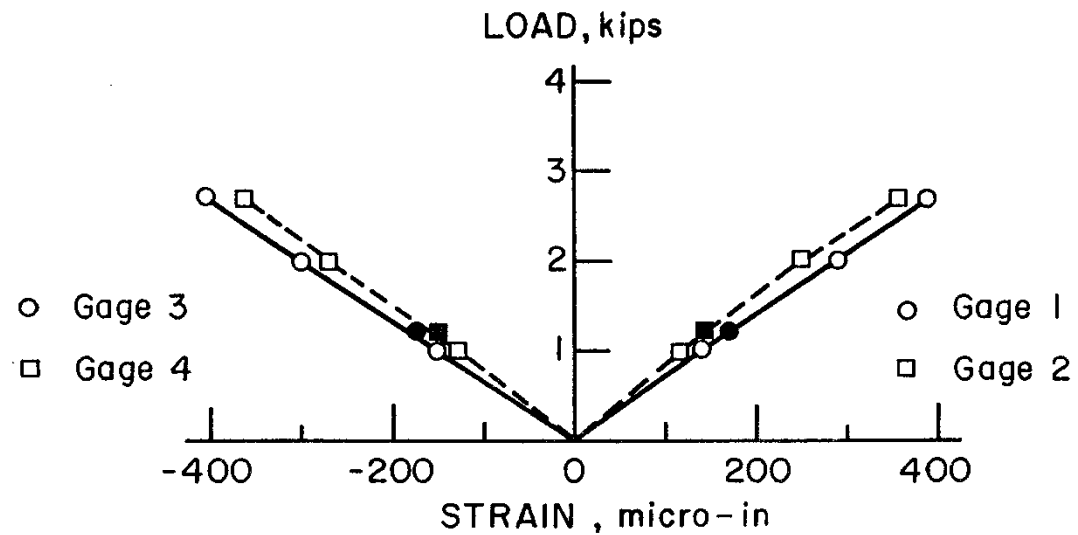


Fig. 24 Load-Deflection and Load-Strain Behavior of Specimen V5

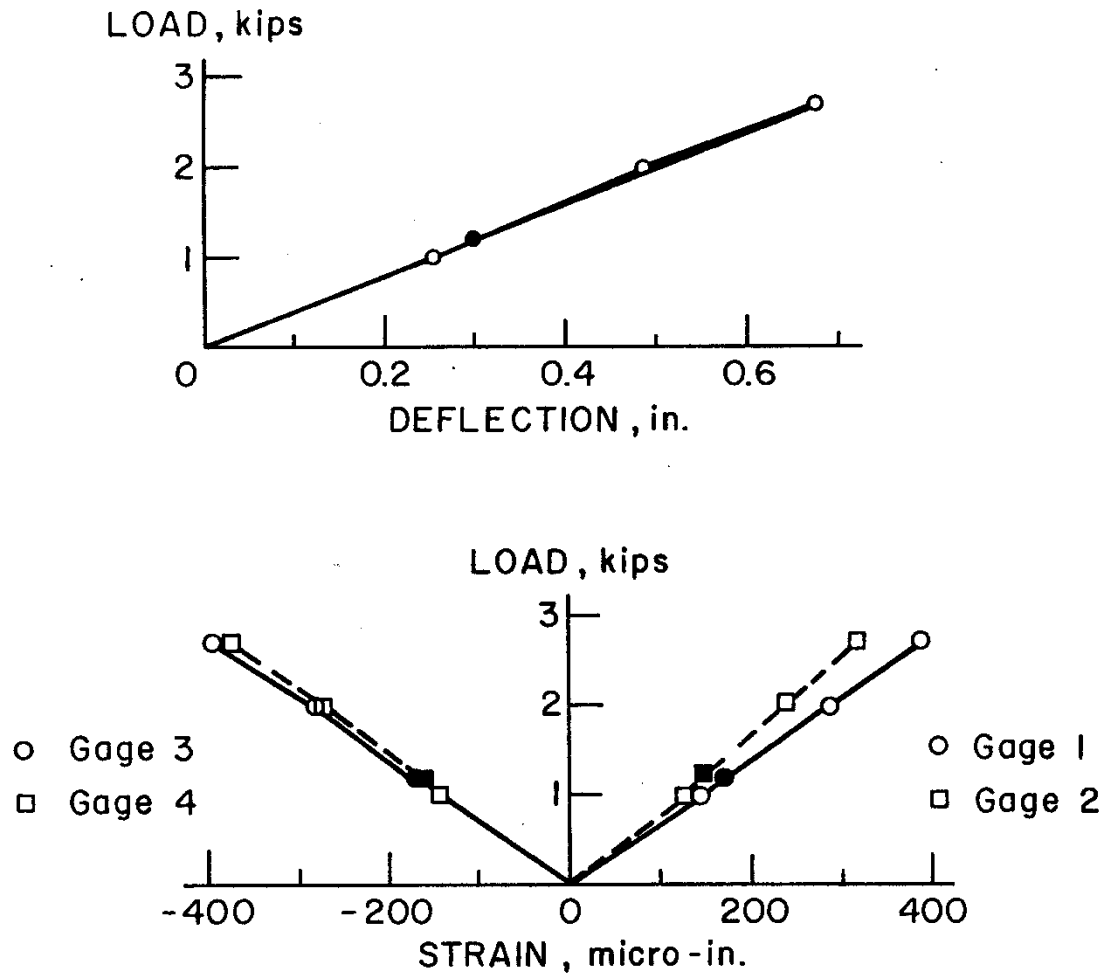


Fig. 25 Load-Deflection and Load-Strain Behavior of Specimen V6

↓ Strain Gage

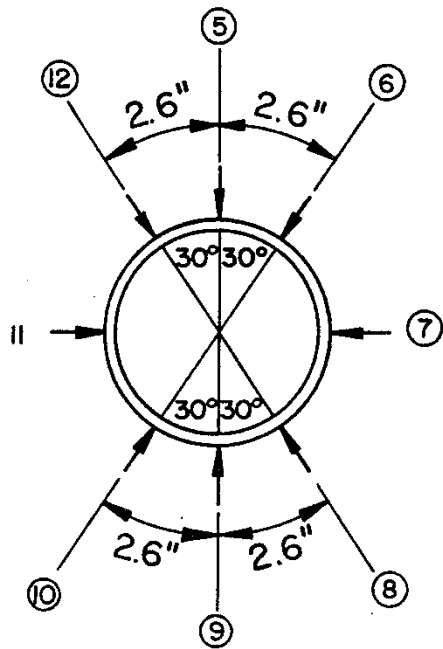
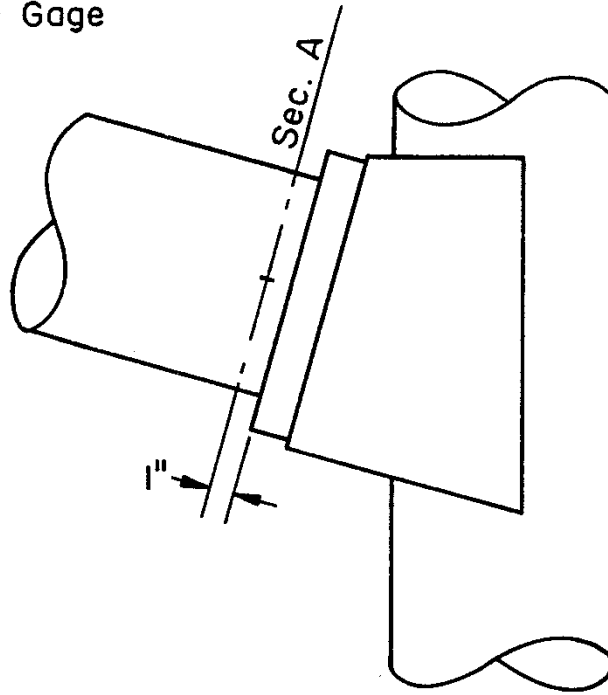


Fig. 26 Location of Strain Gages on Pipe Arm of Specimen V4

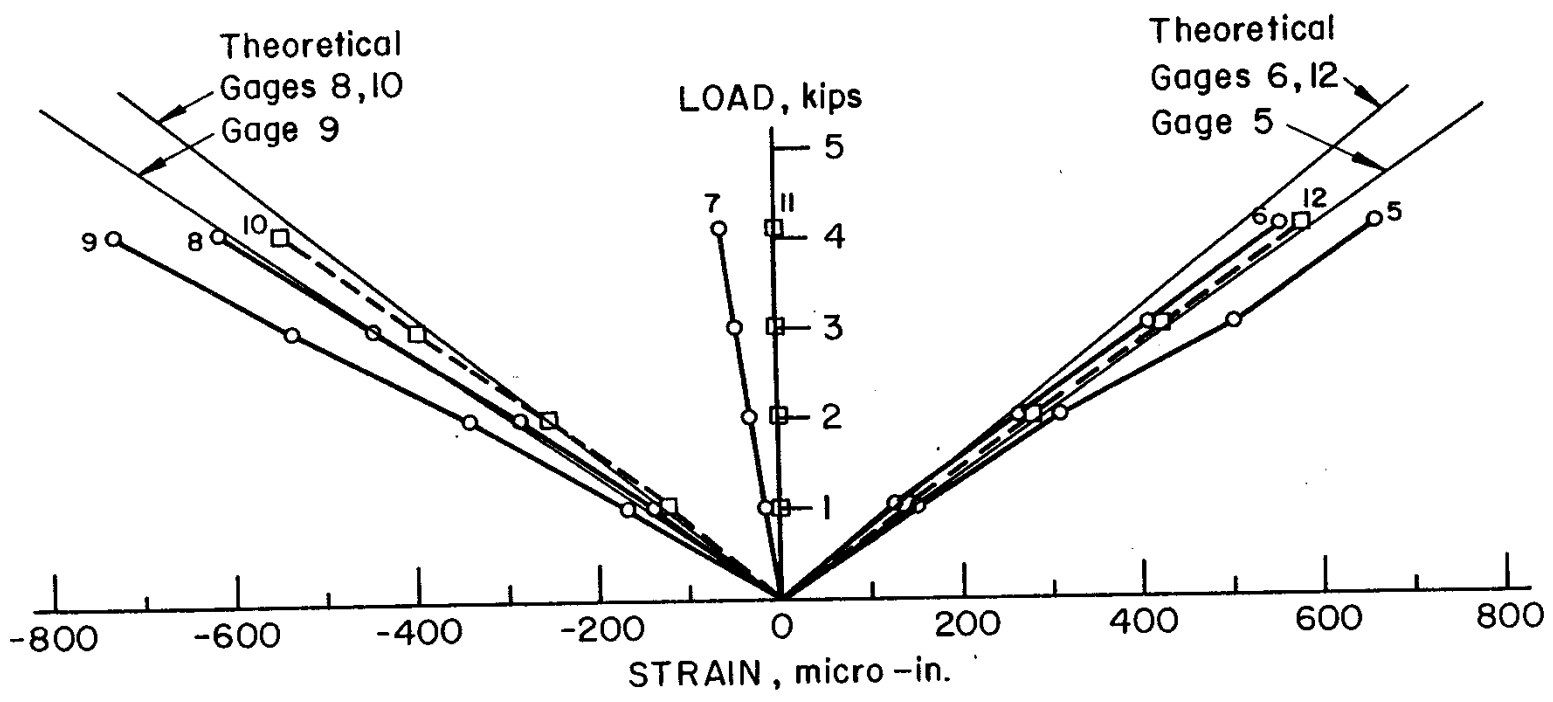


Fig. 27 Load Strain Response Around Pipe Arm - Specimen V4

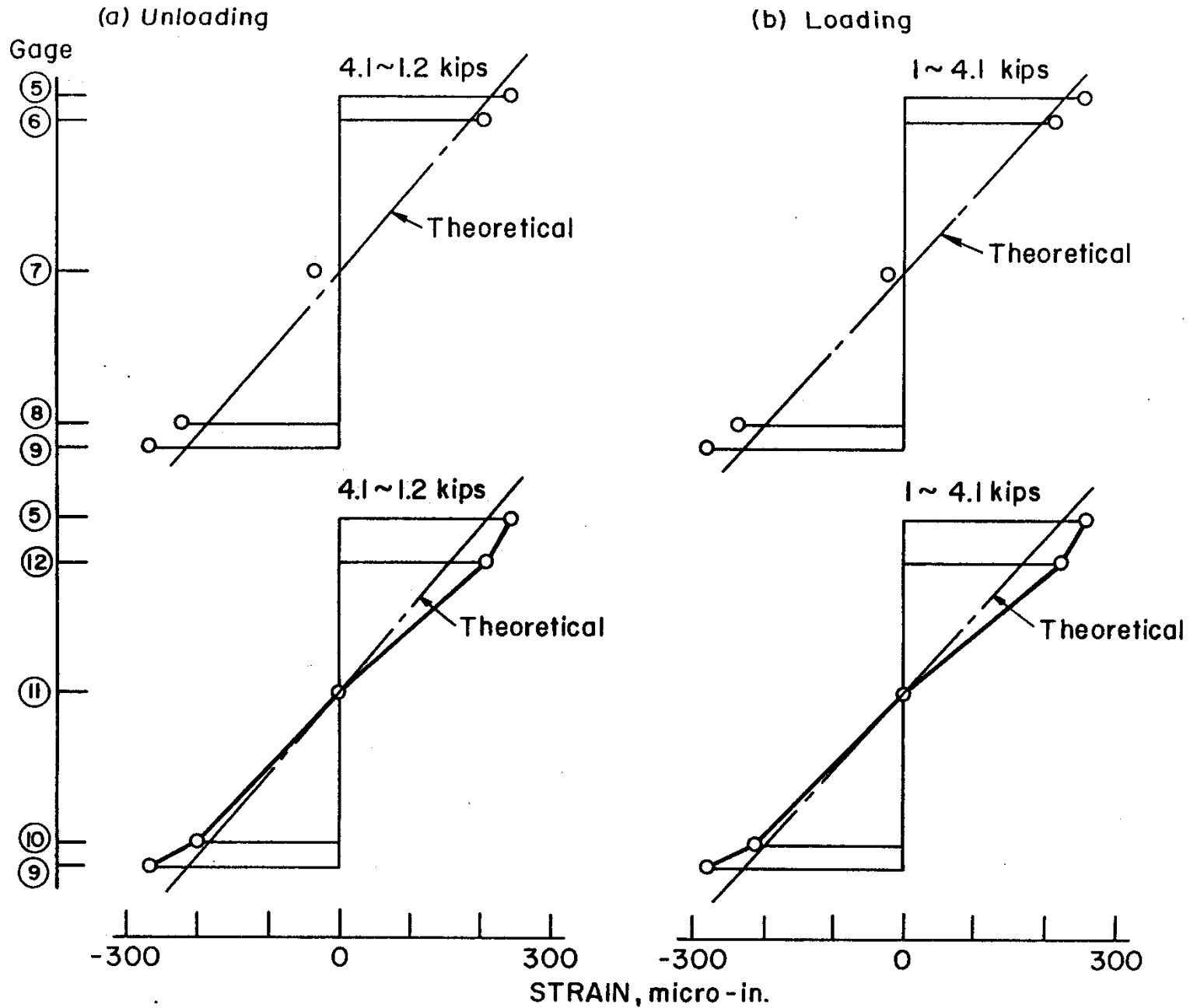


Fig. 28 Comparison of Measured Strain Distribution with Theoretical Distribution, Specimen V4

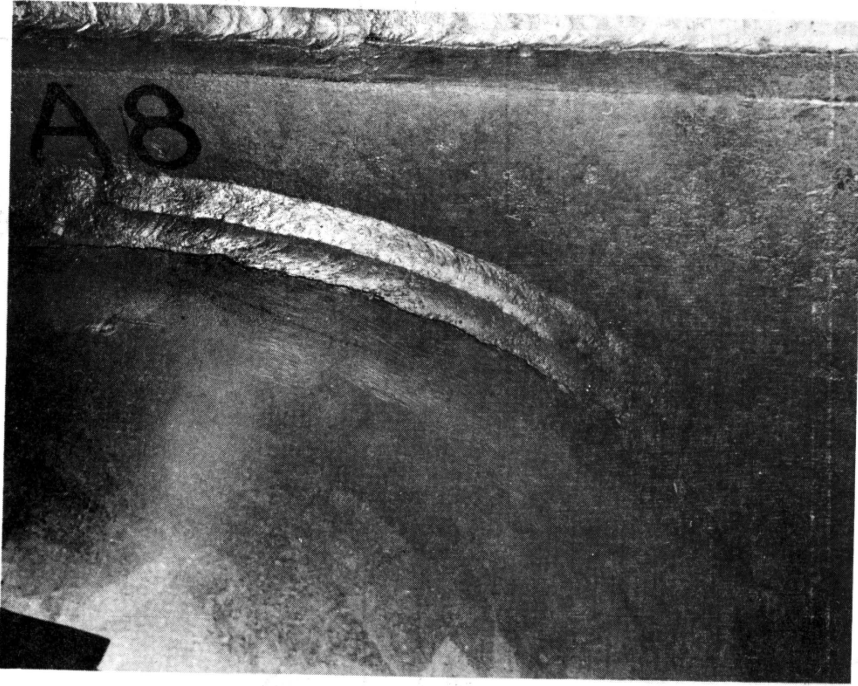


Fig. 29 Typical Crack at Weld Toe on Pipe Arm

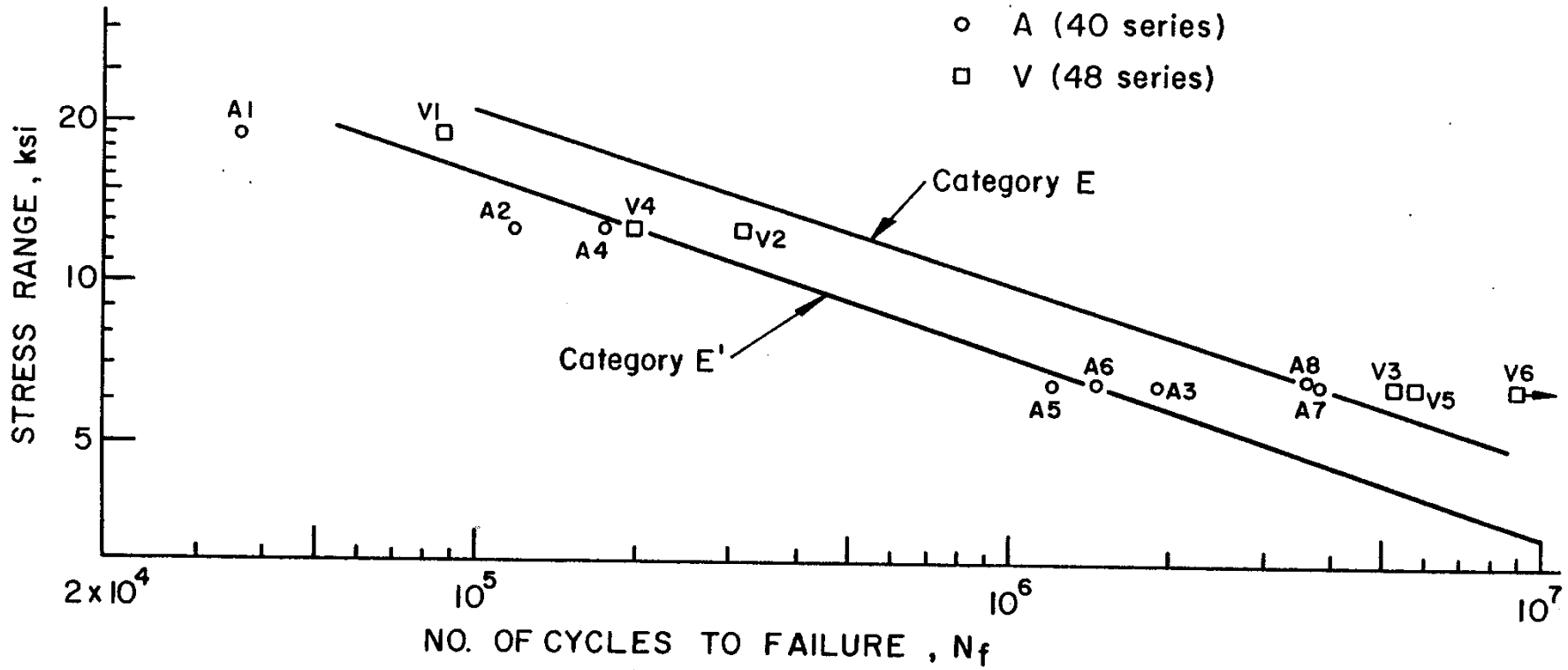
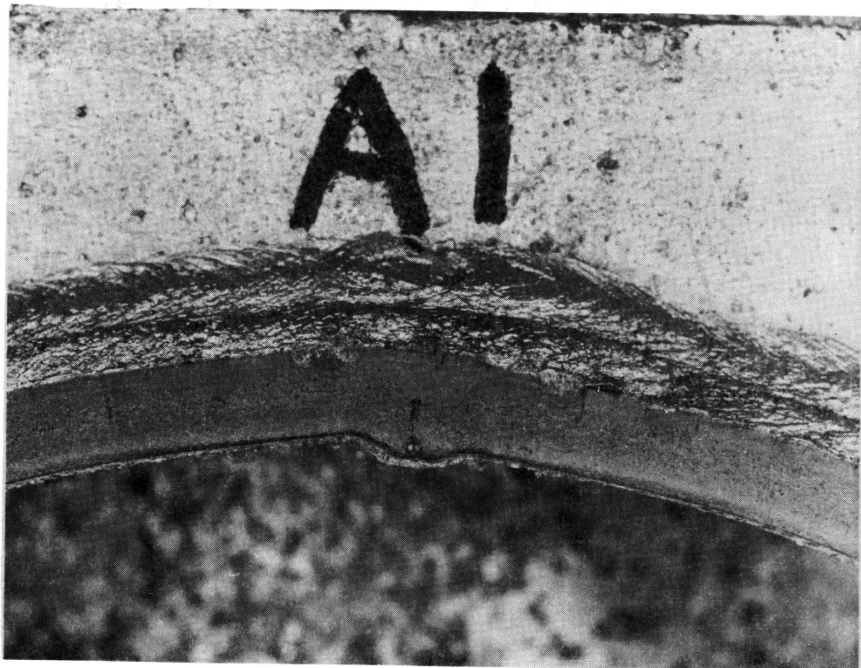


Fig. 30 Summary of Stress Range versus Cycle Life for A and V Series

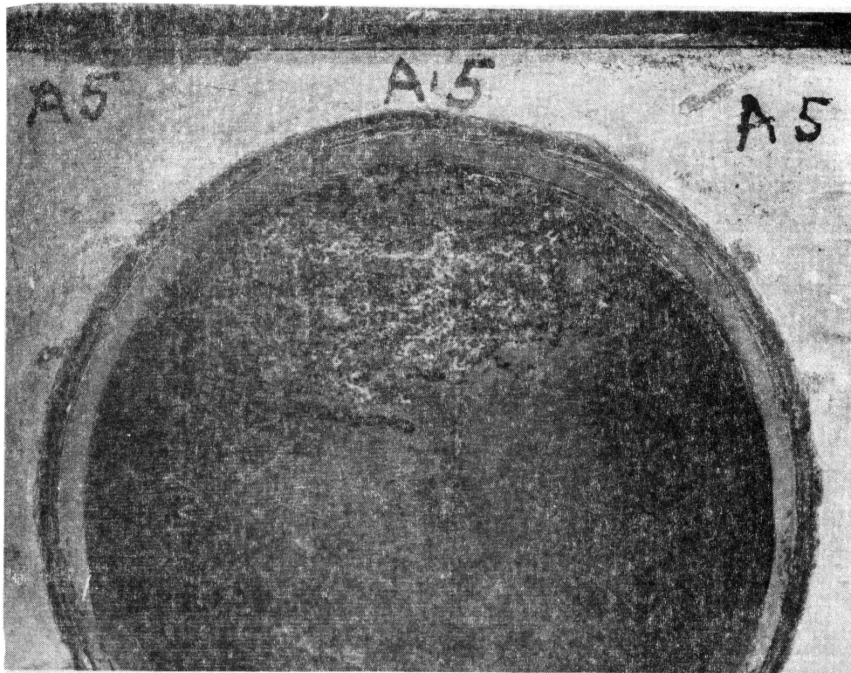


(a) Overview of Fatigue Crack Surface at Arm



(b) Close-up Showing Crack Surface Near Primary Crack Initiation Site

Fig. 31 Crack Surface of Specimen A1

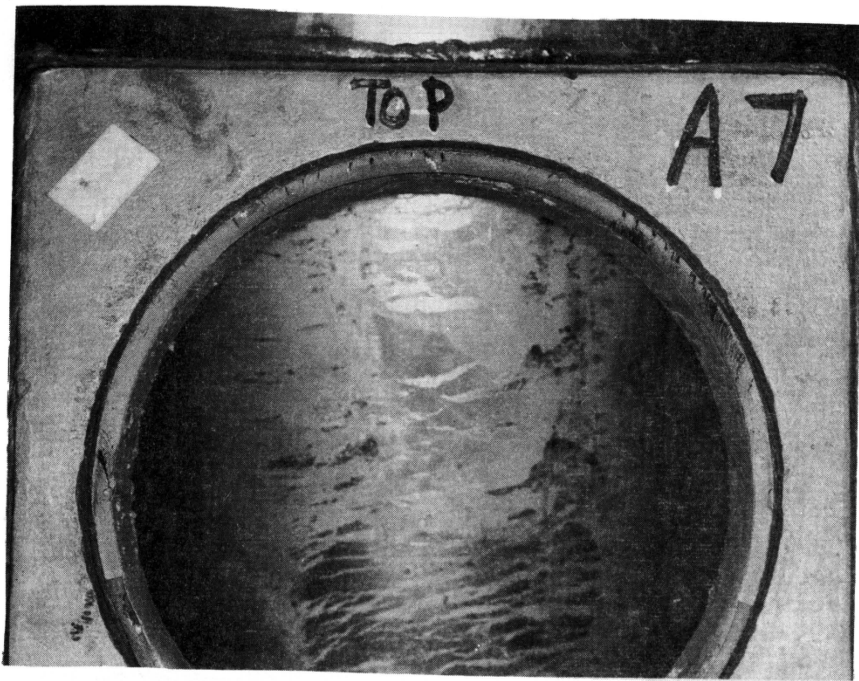


(a) Overview of Fatigue Crack Surface at Arm

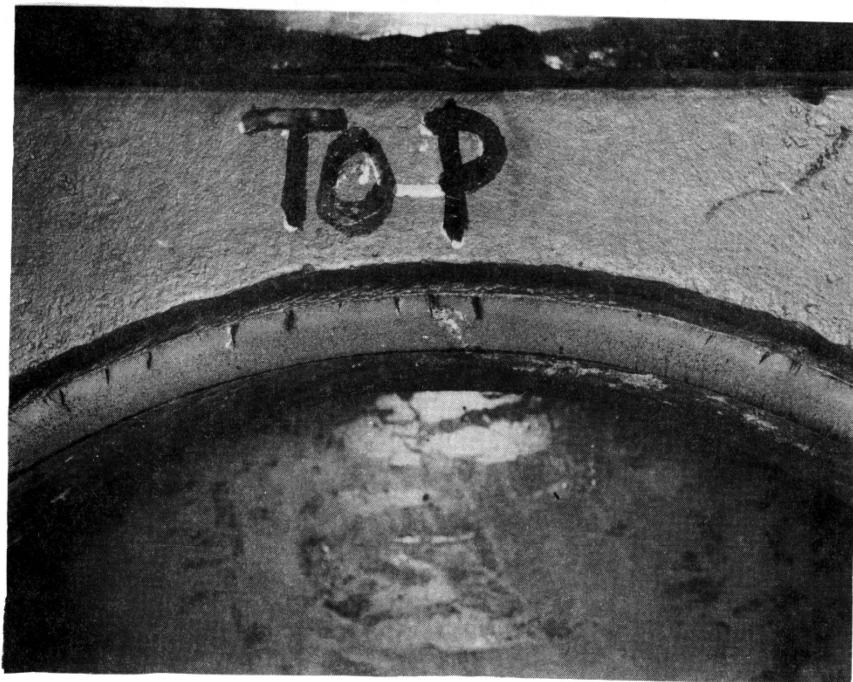


(b) Close-up of Crack Surface Near Primary Crack Initiation Site

Fig. 32 Crack Surfaces of Specimen A5

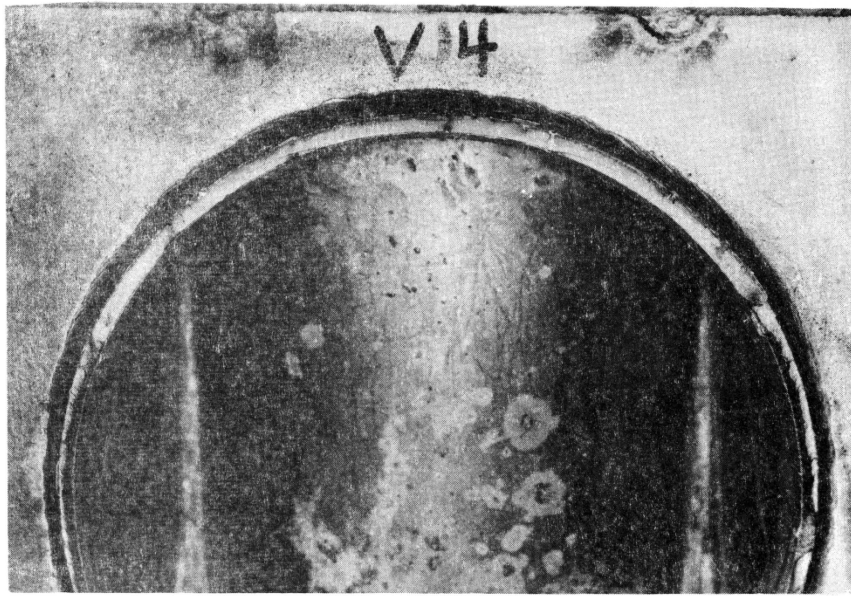


(a) Overview of Fatigue Crack Surface at Arm



(b) Close-up View of Crack Surface at Primary Initiation Site

Fig. 33 Crack Surfaces of Specimen A7

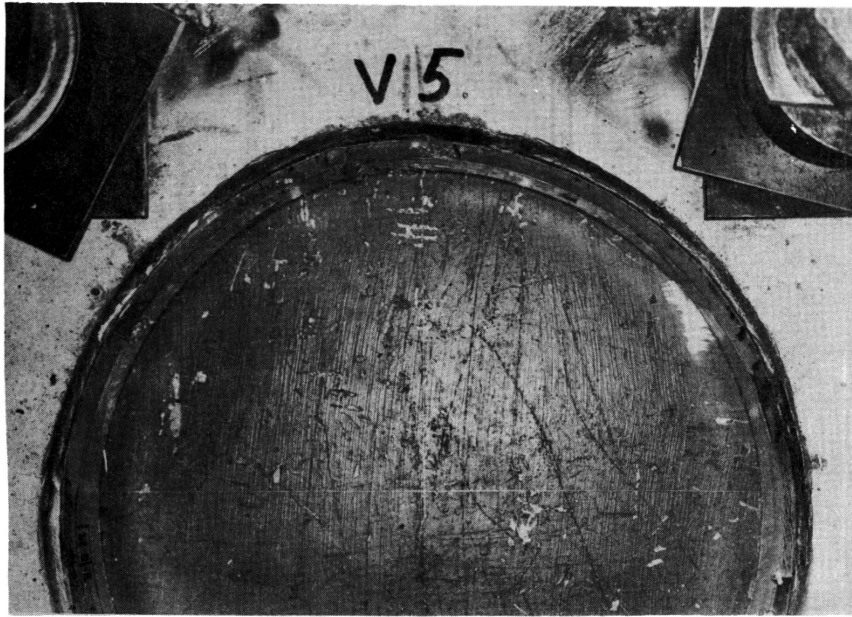


(a) Overview of Fatigue Crack Surface at Arm



(b) Close-up View of Crack Surface at Primary Initiation Site

Fig. 34 Crack Surfaces of Specimen V4



(a) Overview of Fatigue Crack Surface at Base



(b) Close-up View of Crack Surface at Primary Initiation Site

Fig. 35 Crack Surfaces of Specimen V5

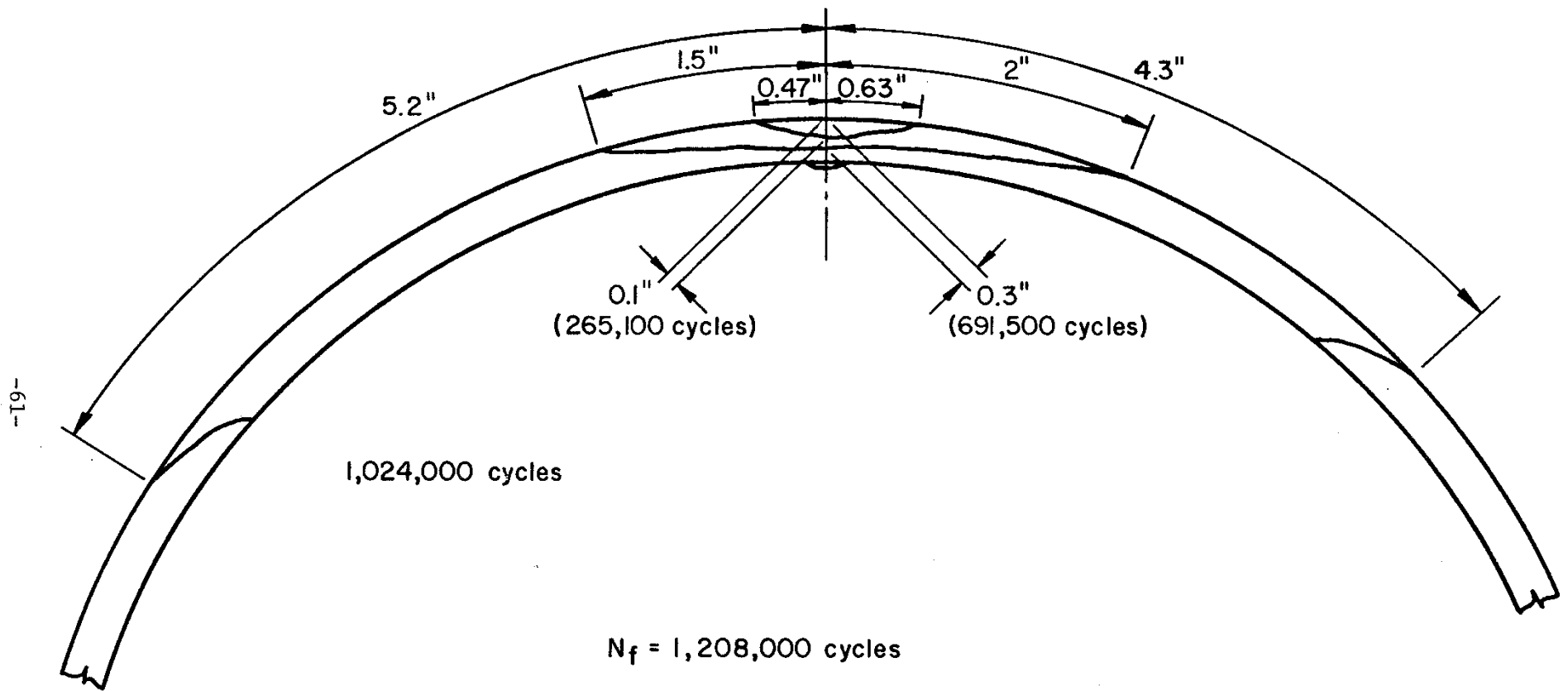


Fig. 36 Crack Shape at Various Cycle Life Intervals - Specimen A5

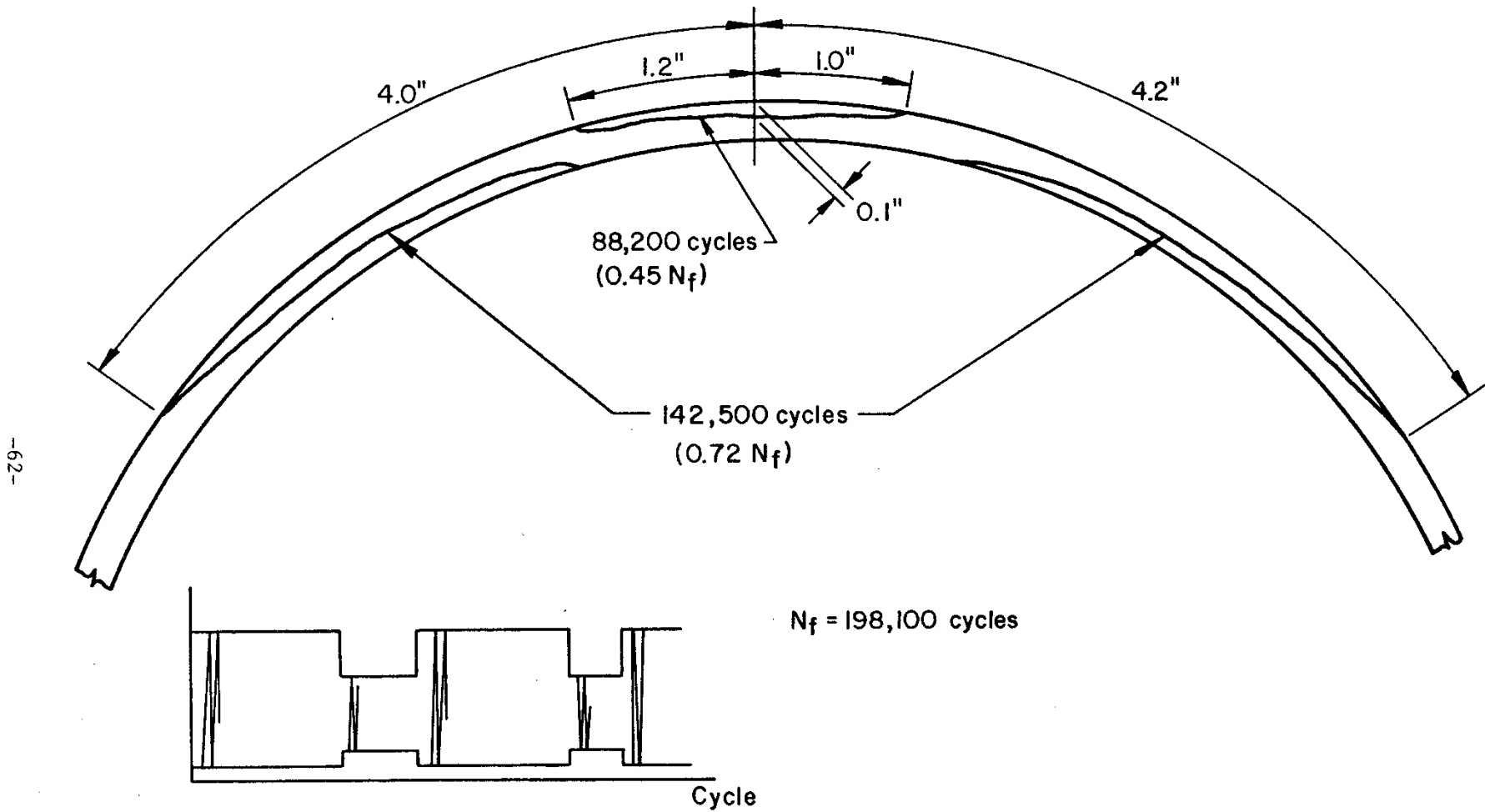


Fig. 37 Crack Shape at Various Cycle Life Intervals - Specimen V4

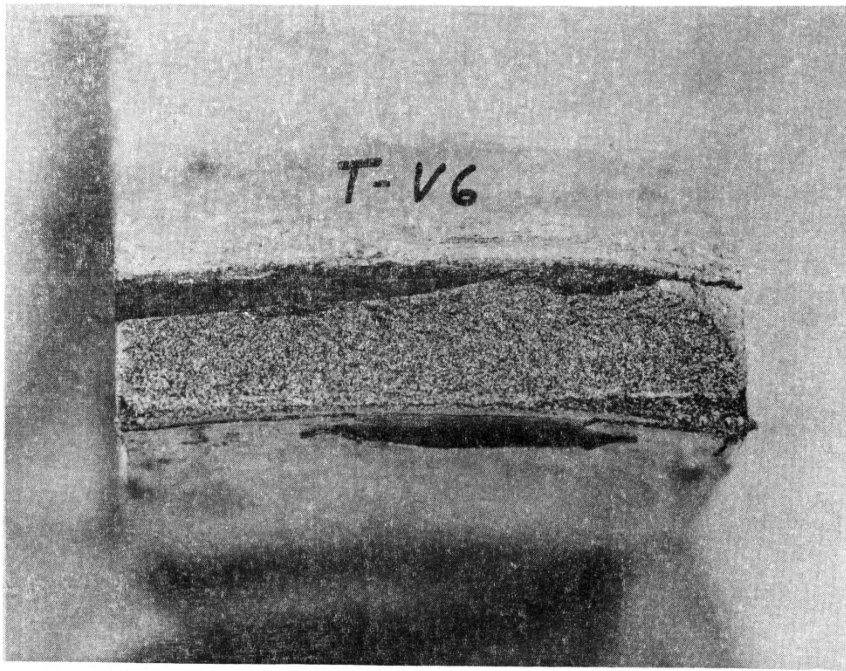


Fig. 38 Fatigue Crack Detected at the Pipe Arm Weld
Toe of Specimen V6

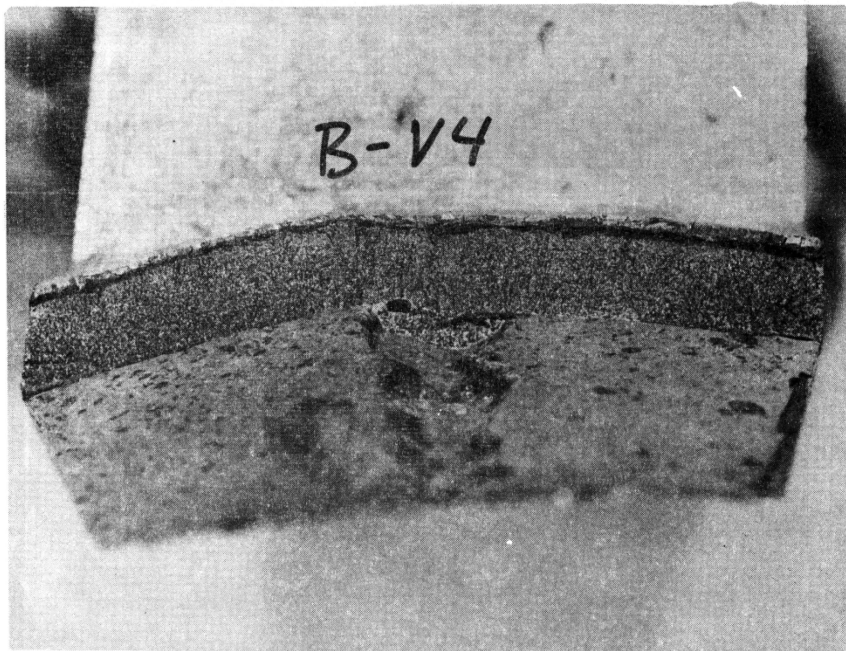
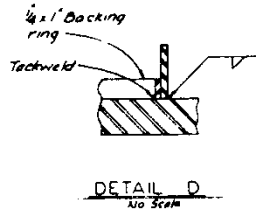
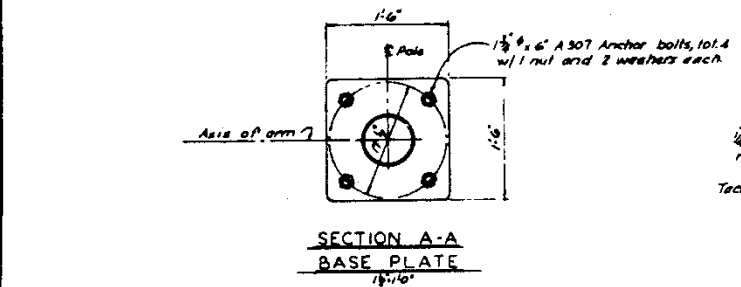
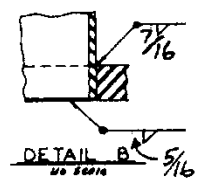
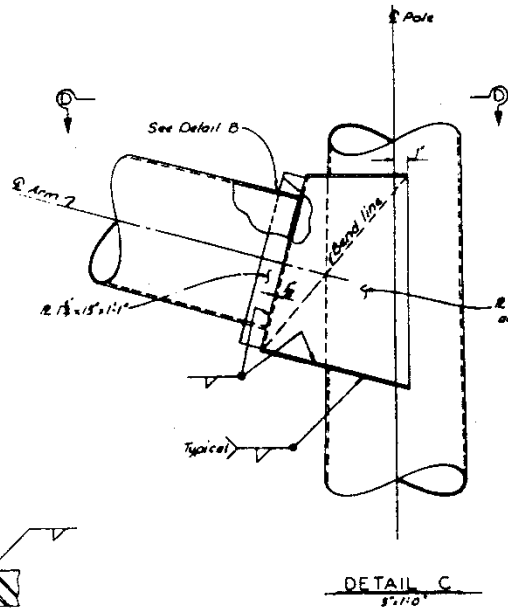
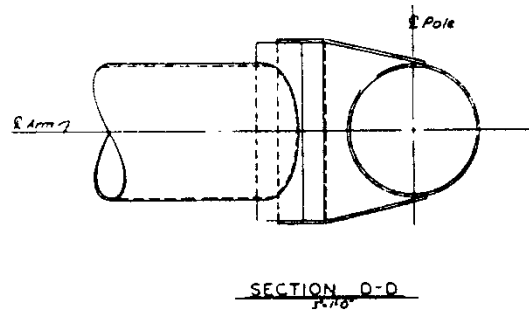
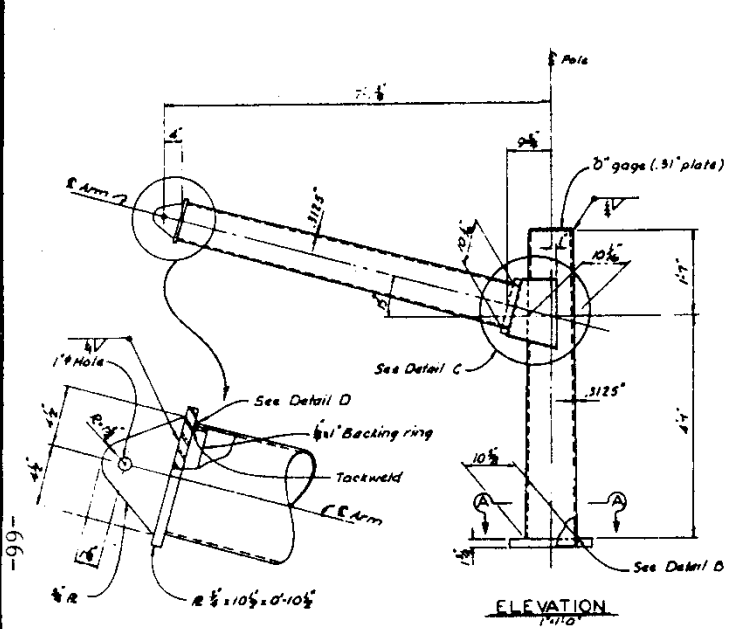


Fig. 39 Small Fatigue Cracks at the Column Base Weld
Toe of Specimen V4



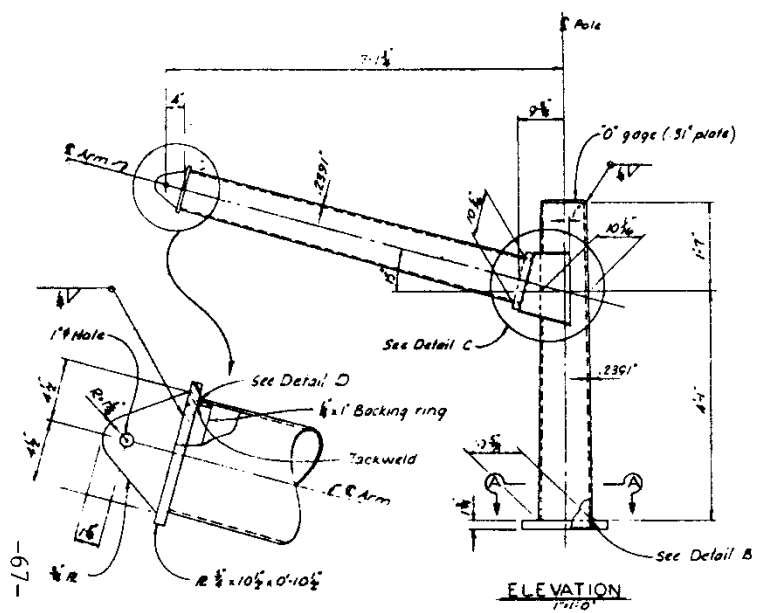
Fig. 40 Small Fatigue Crack at the Column Base Weld
Toe of Specimen A6

APPENDIX I

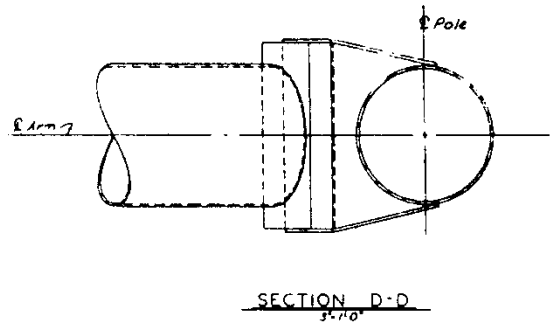


- Notes:
1. Steel ASTM A-285 grade D minimum yield 40,000 psi after fabrication. Bolts/nuts after fabrication.
 2. Tube taper .1875/ft.
 3. Arm connection plates are 3/16" (0" gage) unless noted otherwise. Use maximum fillet weld size.
 4. All welding shown shall conform to AWS D1.1, "Structural Welding Code - Steel"

DESIGN: Riker 7-77 DRAWN: J. R. ... QUANTITY:	CHECKED: Ben Malone 1/29 DATE: 1-29 BY: Ben Malone (H)	State of CALIFORNIA DEPARTMENT OF TRANSPORTATION	STRUCTURES - DESIGN 4 PROJECT ENGINEER: Eng. Riker 7-910	DRAWING NO.: TEST FILE:	POLE FATIGUE TEST TEST SPECIMEN 40 SERIES (6 REQUIRED)	CHECKED BY: _____ DATE: _____
---	--	---	---	----------------------------	---	----------------------------------

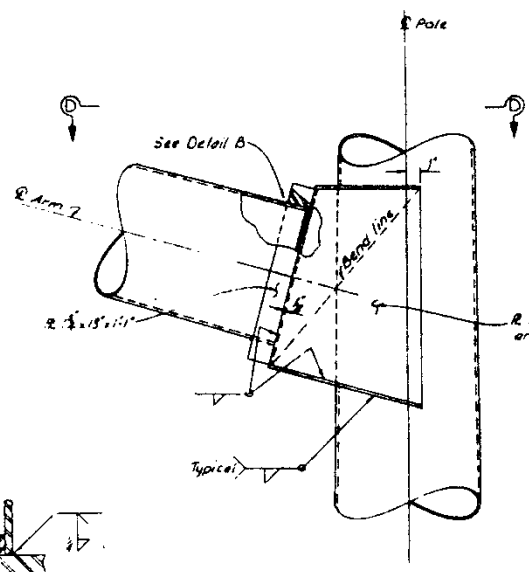


ELEVATION
1 1/2" = 1'-0"

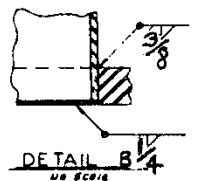


SECTION D-D
3'-11 1/2"

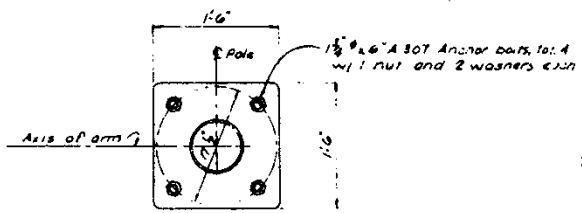
REDUCED PLAN
USE SCALE BELOW
1" = 3'-0" OF ORIGINAL PLAN



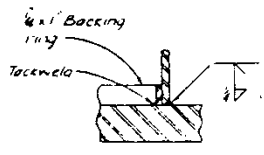
DETAIL C
3'-11 1/2"



DETAIL B
1/4" = 1'-0"



SECTION A-A
BASE PLATE
1 1/2" = 1'-0"



DETAIL D
1/4" = 1'-0"

- Notes:**
1. Steel ASTM A-555 grade A minimum yield 48000 psi after fabrication. Galvanize after fabrication.
 2. Tube taper .375"/ft.
 3. Arm connection plates are .31" (0" gage) unless noted otherwise noted. Use maximum fillet weld size.
 4. A. W. D. T. SHOWS SHALL conform to AWS D. 1.1, Structural Welding Code-Steel

DESIGNER: <i>R. H. Reynolds</i>	DATE: <i>7-72</i>	PROJECT: <i>POLE FATIGUE TEST</i>	STATE OF CALIFORNIA DEPARTMENT OF TRANSPORTATION	STRUCTURES - DESIGN 4	PROJECT NO.: _____	TEST SPECIMEN 4B SERIES (6 REQUIRED)
DETAILS: <i>J. Reynolds</i>	SCALE: <i>1/4" = 1'-0"</i>	APPROVED: _____	CHECKED: _____	DESIGNED BY: _____	DATE: _____	

ALL DIMENSIONS IN INCHES
FOR REDUCED PLAN

CU
WO

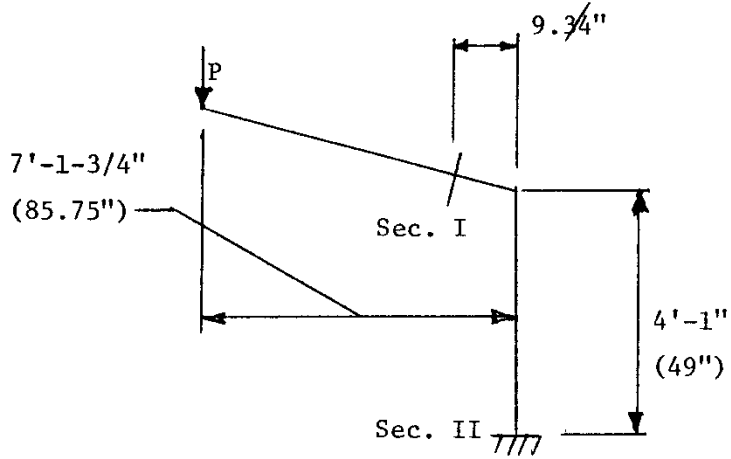
Discharge prior to being marked and sealed.

7/72

APPENDIX II

STRESS ANALYSIS OF POLES

1. Bending Moment

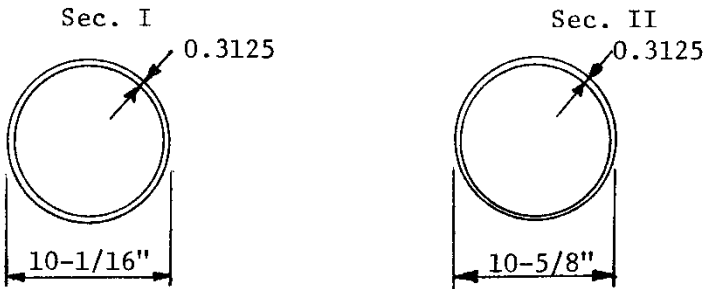


Section I: $M = (85.75'' - 9.75'') \times P$
 $= 76 P$ [kilo-pounds-inch]

Section II: $M = 85.75 P$

2. Moment of Inertia

1. 40 Series



$$I = \frac{\pi}{64} (D_1^4 - D_2^4)$$

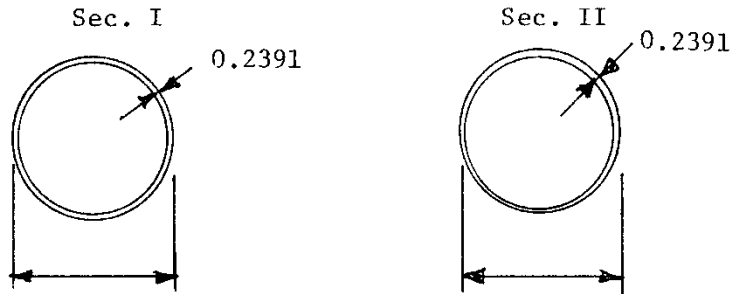
$$I = \frac{\pi}{64} (10.0625^4 - 9.4375^4)$$

$$= 113.86 \text{ [inch}^4\text{]}$$

$$I = \frac{\pi}{64} (10.625^4 - 10^4)$$

$$= 134.71 \text{ [inch}^4\text{]}$$

2. 48 Series



$$I = 89.06 \text{ [inch}^4\text{]}$$

$$I = 105.24 \text{ [inch}^4\text{]}$$

$$E = 29,000 \text{ ksi}$$

3. Bending Stress

1. 40 Series

$$\begin{aligned} \text{Sec. I: } \sigma_b &= \frac{M}{I} y \\ &= \frac{76 \cdot P}{113.86} \times \frac{10.0625}{2} \\ &= 3.358 P \quad \text{[ksi]} \end{aligned}$$

$$\begin{aligned} \text{Sec. II: } \sigma &= \frac{85 \cdot 75P}{134.71} \times \frac{10.625}{2} \\ &= 3.382 \cdot P \quad \text{[ksi]} \end{aligned}$$

2. 48 Series

$$\begin{aligned} \text{Sec. I: } \sigma &= \frac{76 \cdot P}{89.06} \times \frac{10.0625}{2} \\ &= 4.293 \cdot P \quad \text{[ksi]} \end{aligned}$$

$$\begin{aligned} \text{Sec. II: } \sigma &= \frac{85 \cdot 76P}{105.24} \times \frac{10.625}{2} \\ &= 4.329 \cdot P \quad \text{[ksi]} \end{aligned}$$

4. Stress by Axial Force at Sec. II

1. 40 Series

Sec. II Area (A)

$$A = \frac{\pi}{4} (10.625^2 - 10^2)$$
$$= 10.12 \text{ (in.}^2\text{)}$$

$$\therefore \sigma_{ax} = \frac{P}{10.12}$$

2. 48 Series

Sec. II $A = \frac{\pi}{4} (10.625^2 - 10.1468^2)$

$$= 7.8 \text{ (in.}^2\text{)}$$

$$\therefore \sigma_{ax} = \frac{P}{7.8}$$